HETEROCYCLES, Vol. 102, No. 3, 2021, pp. 419 - 450. © 2021 The Japan Institute of Heterocyclic Chemistry
Received, 29th June, 2020, Accepted, 2nd September, 2020, Published online, 8th September, 2020
DOI: 10.3987/REV-20-938

9,9'-BI(XANTHENE)-TYPE HEXAPHENYLETHANE DERIVATIVES AS ADVANCED ORGANIC ELECTROCHROMIC SYSTEMS

Takanori Suzuki,[a]* Yusuke Ishigaki,[a] Masaki Takata,[a] Jun-ichi Nishida,[b] and Takanori Fukushima[c]

In memory of Hidetoshi Yamada and Jun-ichi Yoshida

[a]Department of Chemistry, Faculty of Science, Hokkaido University, Sapporo, Hokkaido 060-0810, Japan. [b]Department of Applied Chemistry, Graduate School of Engineering, University of Hyogo, Himeji 671-2280, Japan. [c]Laboratory for Chemistry and Life Science, Institute of Innovative Research, Tokyo Institute of Technology, Yokohama 226-8503, Japan

Abstract – 9-Phenylxanthenyl radical can undergo facile C-C bond formation at C9-position when the two units of the radical are connected at C2'-positions to give stable intramolecular dimer (**1**), which is a clamped hexaphenylethane derivative with an elongated C-C bond. The newly formed bond in **1** can be cleaved easily upon two-electron oxidation to give bis(9-xanthenylium)-type dication ($\mathbf{2}^{2+}$), from which the diradical is generated upon two-electron reduction. This review account describes the dynamic redox ("dyrex") pair of colorless **1** and yellow-orange $\mathbf{2}^{2+}$, which provides a versatile scaffold to develop multi-functional electrochromic systems. Both of **1** and $\mathbf{2}^{2+}$ are sterically challenged molecules and thus adopt characteristic skewed geometries. Electrochiroptical response was realized by suppressing the chiral inversion of helicity in **1** and axial chirality in $\mathbf{2}^{2+}$ whereas redox-induced fluorescence switching was attained by attaching the fluorophore whose emission is quenched by xanthenylium in $\mathbf{2}^{2+}$ but not by spiro(xanthene) unit in **1**. By the molecular design that allows intramolecular chiral transmission, the spectral changes were also induced by the external stimuli (e.g. heat, pH) other than redox input, which made it possible to construct less well-explored multi-input-multi-output response systems. More advanced functions could be endowed, such as chiral redox memory or reversible O_2-storage, by further modification of the prototype.

CONTENTS

1. Introduction

9-Phenylxanthenylium (**I**) is the common skeleton for the many xanthene dyes such as Rhodamine B, which have been widely used as laser dyes[1] or for dye-sensitized solar cells.[2] One-electron reduction of **I** causes formation of the corresponding radical (**II**) (Scheme 1),[3] which has been attracted as a scaffold to generate the thermodynamically stable and kinetically persistent radicals.[4-6] As the end product of **II**, 9,9'-diphenyl-9,9'-bi(xanthene) (**III**) had been postulated,[4] however, it was revealed that **II** does not form

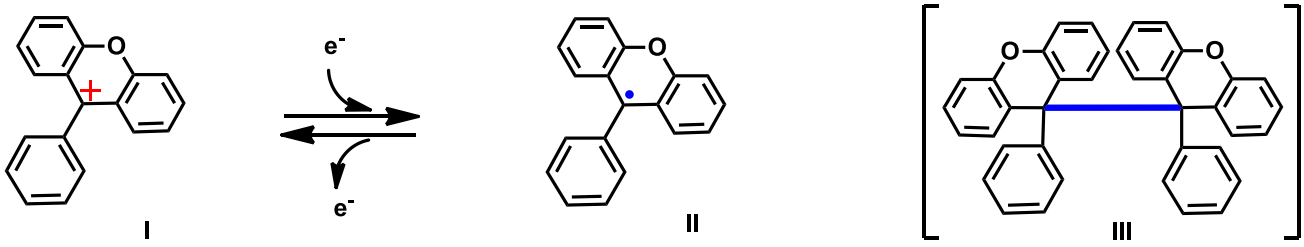

Scheme 1

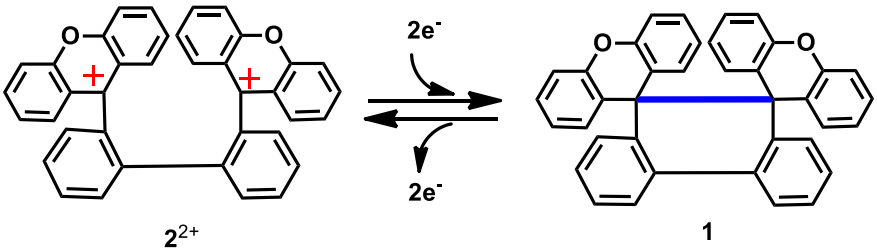

Scheme 2

dimer **III**.[6] The lack of dimerization obviously comes from the severe steric repulsion around the central C-C bond in **III**, which is inherited from hexaphenylethane (HPE).[7-9]

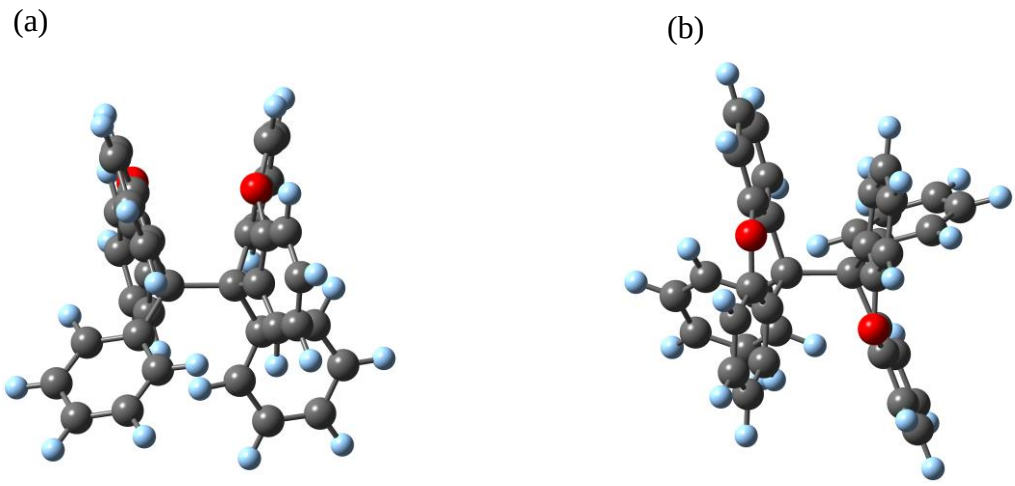

Figure 1. Calculated geometry of **III** by DFT method [B3LYP/6-31G(d)]: (a) side view, (b) top view

According to our DFT calculation[10] on one of the energy-minimized conformers of **III** (torsion angle of C_{Ph}-C_9-C_9-C_{Ph}: 54.5°), the central C-C bond length (*d*) is predicted to be 1.704 Å, which is much longer than the standard (1.54 Å)[11] but close to the calculated value for that of parent HPE (1.735 Å) (Figure 1).[10,12] Based on the proposed linear correlation between the bond dissociation energy and *d*,[13] the bond fission of **III** would occur very easily unless the additional interaction (e.g. dispersion force)[9] between the two phenylxanthene units can help suppressing the bond dissociation, as in the case of bis(diamondoid) compounds that have the longest C_{sp3}-C_{sp3} bond among the alkanes without C_{sp2} carbons.[14]

On the other hand, we envisaged that more reliable method to stabilize **III** is clamping[15-17] the two phenyl rings. Thus, dispiro[xanthene-9,9'(9'*H*,10'*H*)-phenanthrene-10',9"-xanthene] (**1**) was designed as a stable and persistent HPE derivative, in which an extra C-C bond is made in the structure of dimer (**III**). Actually, the dication ($\mathbf{2}^{2+}$) with two units of 9-phenylxanthenylium connected at the C2' position undergoes facile C_9-C_9 bond formation to give **1** upon two-electron (2e) reduction. It should be noted that the newly formed bond of **1** can be cleaved to regenerate dication ($\mathbf{2}^{2+}$) when treated with two equivalents of a one-electron oxidant (Scheme 2),[18] so that **1** and $\mathbf{2}^{2+}$ can consist of a kind of "reversible" redox pair. This review account describes the novel electrochromic systems based on the interconvertible pair of colorless **1** and yellow-orange $\mathbf{2}^{2+}$, which can serve as a versatile scaffold to develop advanced molecular response systems.

2. Dihydrophenanthrene with two units of spiro(xanthene): A prototype of the dyrex system

The significant difference between the two reaction schemes for the monomeric and dimeric 9-phenylxanthenyliums shown in Schemes 1 and 2 is that the chemical process (C-C bond formation) is followed by 2e-transfer during the reduction process in the latter (EEC mechanism[19]). The detailed study on the related molecules showed that the oxidation process in the latter involves ECE mechanism,[19] and thus the bond cleavage occurs just after the 1e-transfer (Scheme 3).[18] The interconvertible pair undergoing reversible C-C bond formation/cleavage upon 2e-transfer has been categorized as "dyrex (dynamic redox)" systems,[20] for which the pair of **1** and $\mathbf{2}^{2+}$ serves as a representative example. The large separation of redox peaks (E^{ox} of **1** = + 1.42 V and E^{red} of $\mathbf{2}^{2+}$ = +0.50 V vs SCE, respectively, in CH_2Cl_2, peak potentials) as well as 2e-transfer in each wave in the cyclic voltammogram are the often observed features for the dyrex systems (Figure 2).

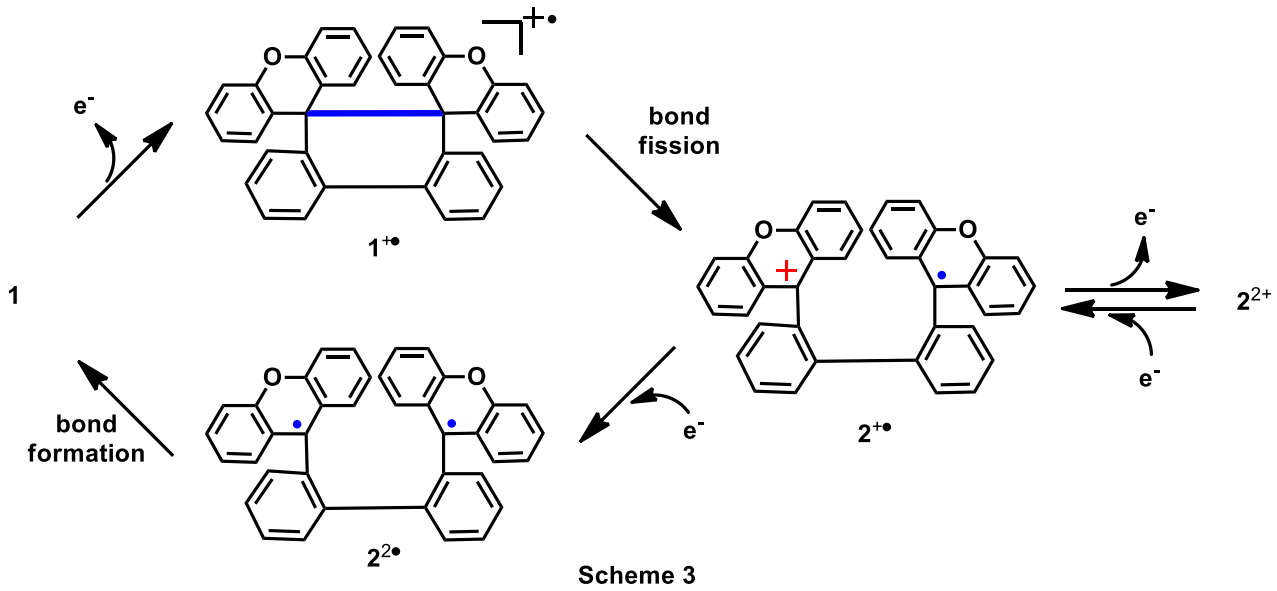

Scheme 3

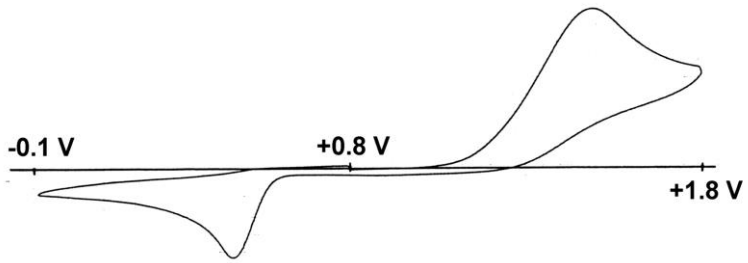

Figure 2. Cyclic voltammogram of $\mathbf{1}/\mathbf{2}^{2+}$ measured in CH_2Cl_2 (E/V vs SCE)

According to the DFT calculation,[10] a dynamic structural change is predicted upon interconversion between **1** and $\mathbf{2}^{2+}$ (Figures 3 and 4). The two 9-xanthenylium units are only partially overlapped in $\mathbf{2}^{2+}$ since the biphenyl unit is twisted by 66.7°, and thus the C9 -- C9 separation (3.79 Å) is much larger than the sum of van der Waals radii of C_{sp2} (3.40 Å).[21] By forming a new C-C bond with transforming to neutral compound **1**, the twisting angle becomes 17.8°, and thus the six C_{sp2} carbons around the newly formed C-C bond are arranged in a sort of eclipsed manner. The "front strain"[16] in the eclipsed geometry is the reason for the great *d* value (1.658 Å) for the central bond in **1**, which is a clamped derivative of HPE with the 9,10-dihydrophenanthrene skeleton.[15,17] At the same time, such a geometrical change as well as the presence/absence of the C-C bond are the reasons for the quite different redox potentials.

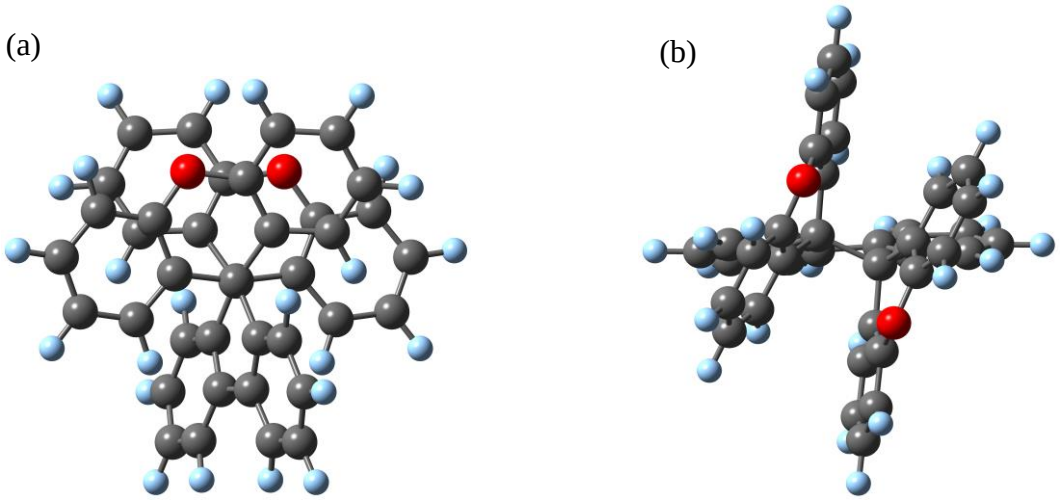

Figure 3. Optimized structures of **1** by DFT method [B3LYP/6-31G(d)]: (a) side view, (b) top view

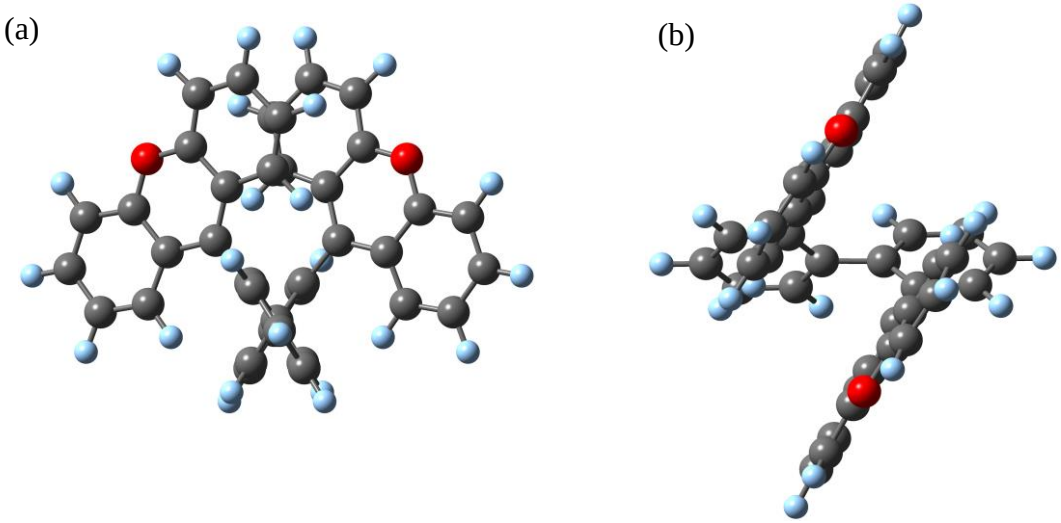

Figure 4. Optimized structures of $\mathbf{2}^{2+}$ by DFT method [B3LYP/6-31G(d)]: (a) side view, (b) top view

The dyrex behavior can be also accounted for by considering their MOs (Figures 5 and 6). In the HOMO of **1**, the orbital coefficients are mainly localized on the electron-donating spiro(xanthene) units, as expected. A considerable coefficient is also found on the central C-C bond due to the "through-bond interaction".[22,23] One-electron oxidation of **1** causes the decrease in bonding character of the C-C bond, leading to the facile mesolysis[24] of the central bond upon 1e-oxidation. In addition, in the LUMO of $\mathbf{2}^{2+}$, the largest coefficients are located at two C9 carbons, whose orbitals are interacting in an in-phase manner between the facing 9-xanthenylium units, which causes C-C bond formation upon receiving electrons in LUMO.

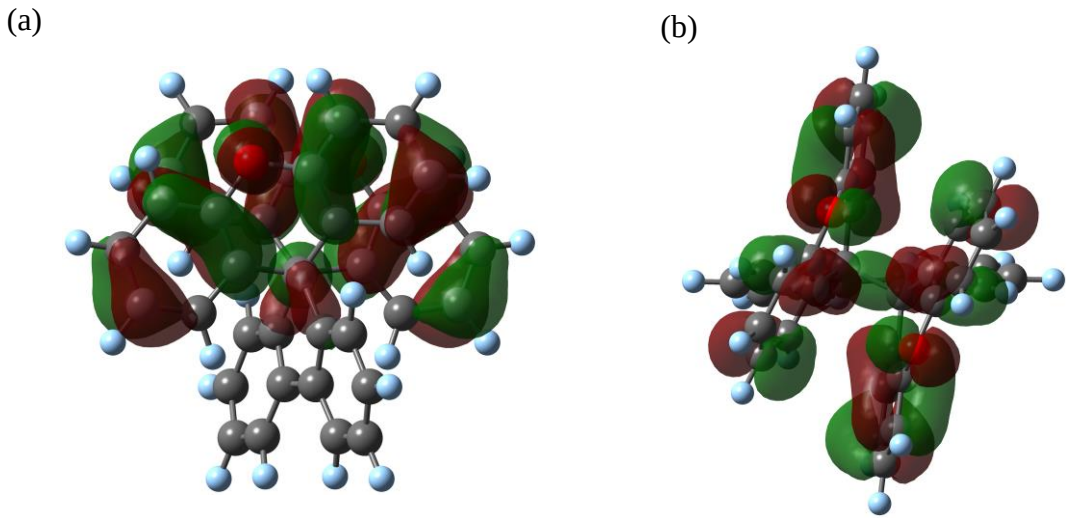

Figure 5. HOMO of **1** by DFT method [B3LYP/6-31G(d)]: (a) side view, (b) top view

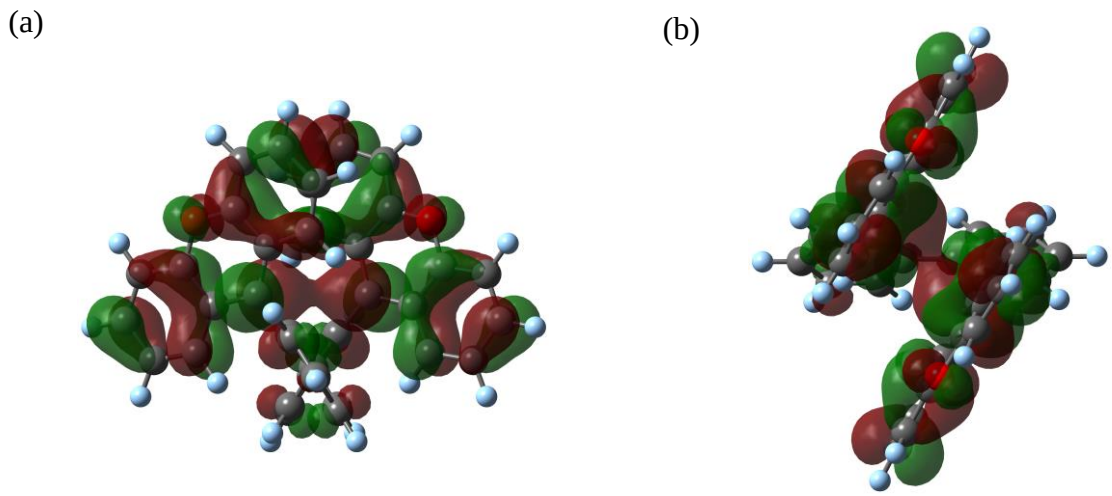

Figure 6. LUMO of $\mathbf{2}^{2+}$ by DFT method [B3LYP/6-31G(d)]: (a) side view, (b) top view

Both of **1** and $\mathbf{2}^{2+}$ are sterically congested molecules. To reduce the steric hindrance, they adopt helical/twisted geometries with C_2-symmetry. However, their ^{1}H NMR spectra exhibit time-averaged signals assigned to the C_{2v}-symmetic species due to rapid ring flip in **1** and free rotation around the biphenyl axis in $\mathbf{2}^{2+}$. VT-NMR analyses indicated that the rotational barrier in the latter is only 12.5 kcal mol^{-1} whereas that for the ring flip in the former is much smaller.[25] On the other hand, by attaching bulky substituents at the bay region of **1** and $\mathbf{2}^{2+}$, optically pure dyrex pair could be obtained, for which stereospecific interconversion would occur only between certain stereoisomers (*vide infra*).

3. Multi-input and multi-output electrochromic systems

3.1 Electrochiroptical response system

Electrochiroptical response systems[26] are endowed with the multi-output function, and thus the electrochemical input can be transduced into two kinds of spectral outputs, i.e., UV–Vis and circular dichroism (CD). The pioneering works[27] had been developed to enhance the CD activity through exciton coupling[28] of two chromophores because only a small amplitude in the CD output is available for chiral redox molecules with a simple asymmetric center ($\Delta\varepsilon < 5$).[29]

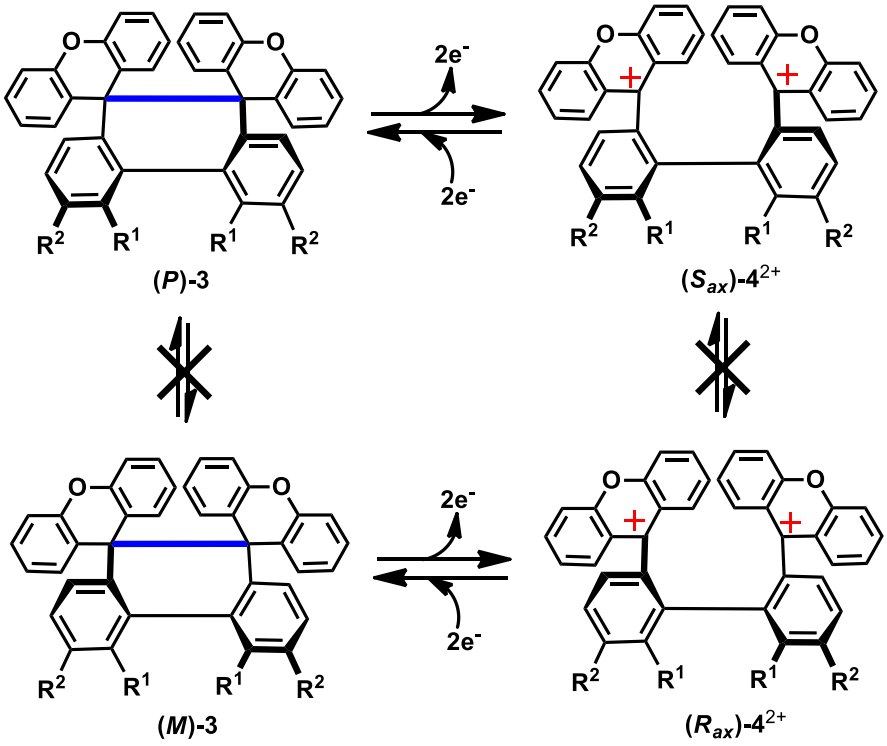

Scheme 4 [a: R^1,R^2 = benzo; b: R^1 = Br, R^2 = H; c: R^1 = Me, R^2 = H]

The helical/twisted geometries of **1** and $\mathbf{2}^{2+}$ are quite suitable for exciton coupling, which prompted us to design new dyrex pairs of **3** and $\mathbf{4}^{2+}$, which would have high racemization barrier to allow optical resolution (Scheme 4). Scheme 5 depicts the synthetic routes for **3a** and $\mathbf{4a}^{2+}$ with a binaphthyl skeleton, in which benzannulation increases steric repulsion in the transition state of racemization. First, racemic 2,2'-dibromobinaphthyl **5** was reacted with BuLi, and the resulting dilithiobinaphthyl was then treated with xanthone to give diol **6a**. Treatment of **6a** with HBF_4 in $(EtCO)_2O$ gave racemic dication salt $\mathbf{4a}^{2+}(BF_4^-)_2$ in quantitative yield, which was converted to **3a** upon reduction with Zn with C-C bond formation, again in quantitative yield. Upon oxidation of **3a** with two equivalents of one-electron oxidant $[(4\text{-}BrC_6H_4)_3N^{+\bullet}\ SbCl_6^-$ (magic blue)], the newly formed bond was cleaved to regenerate $\mathbf{4a}^{2+}$, thus **3a** and $\mathbf{4a}^{2+}$ was shown to be a new entry of dyrex pairs.[30]

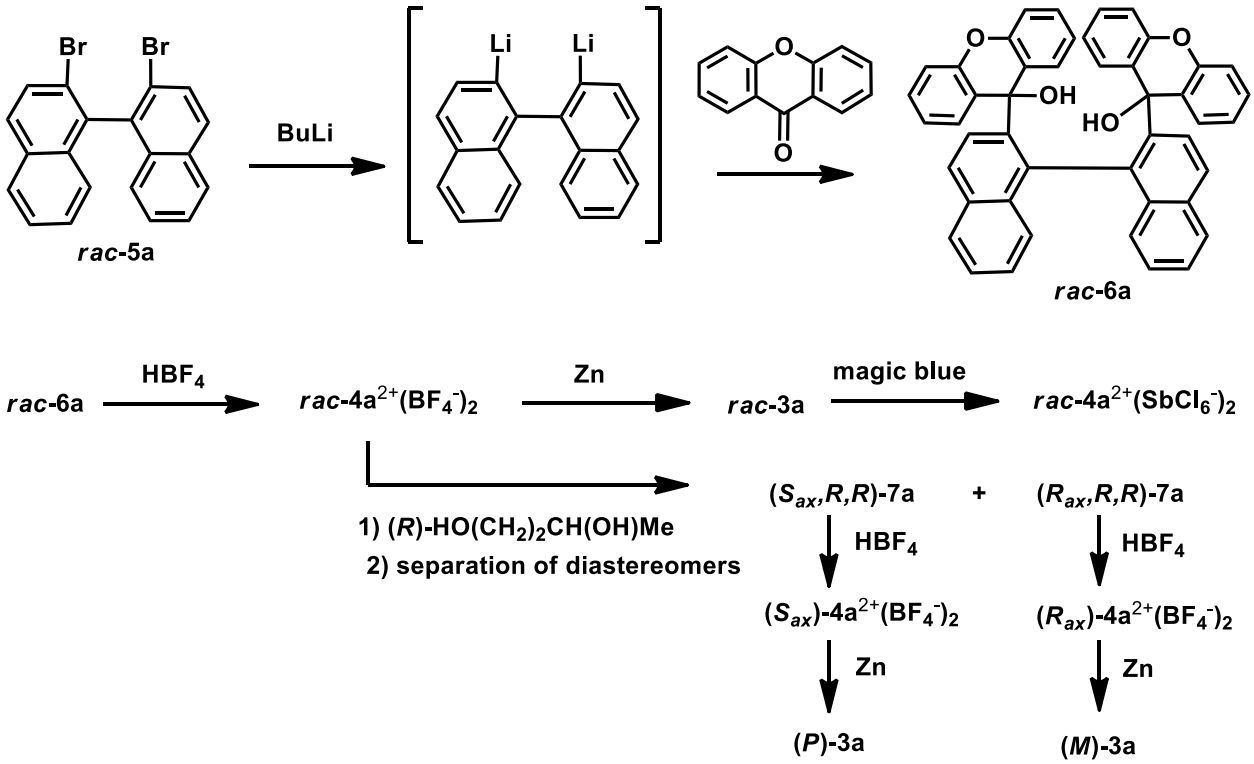

Scheme 5

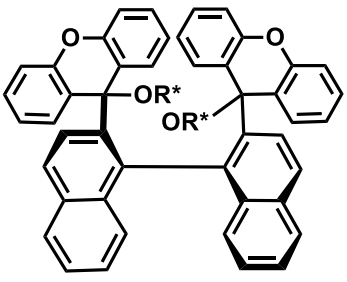

(R_{ax},R,R)-7a
[R* = (*R*)-$(CH_2)_2$CH(OH)Me]

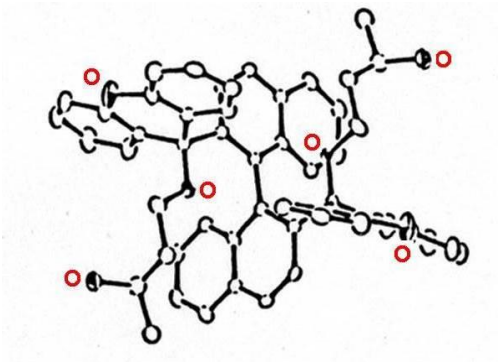

Figure 7. X-Ray structure of (R_{ax},R,R)-**7a**

To resolve the enantiomers, dication salt of *rac*-**4a**$^{2+}$ was reacted with (*R*)-butane-1,3-diol to give a diastereomer mixture of ethers (S_{ax},*R*,*R*)- and (R_{ax},*R*,*R*)-**7a**, the latter of which was analyzed by X-ray to determine its stereochemistry (Figure 7). Acid treatment of (S_{ax},*R*,*R*)- and (R_{ax},*R*,*R*)-**7a** gave optically pure salt of (S_{ax})- and (R_{ax})-**4a**$^{2+}$(BF_4^-)$_2$, respectively, from which (*P*)- and (*M*)-**3a** were obtained selectively upon reduction. They exhibit very large optical rotation {[α]$_D$ +642° for (*P*)-**3a**} due to the helicene-type substructure.[31] Configuration of **3a** and **4a**$^{2+}$ is stable with no sign of racemization at ambient conditions.

Similarly, by starting with selective double lithiation of 2,2',6,6'-tetrabromobiphenyl **5b** (Scheme 6), optically resolved pairs of (*P*)-**3b**/(S_{ax})-**4b**$^{2+}$ and (*M*)-**3b**/(R_{ax})-**4b**$^{2+}$ were obtained, which underwent stereospecific interconversion.[25] Absolute configuration was again confirmed by an X-ray analysis of diastereomeric intermediate of (R_{ax},*R*,*R*)-**7b (**Figure 8). Their configurational stability is attained by the steric bulkiness of bromo groups at the bay region as shown by the X-ray analysis on **3b** (Figure 9). The newly formed C-C bond in **3b** is as long as 1.656(5) Å, which is close to the calculated *d* value of **1**. The twisting angle of biphenyl moiety [41.4(1)º] is larger than that expected for **1**, due to steric repulsion between two bromo groups [Br --- Br: 3.423(1) Å]. Similar twisted structure with a long C-C bond was observed in the X-ray structure of dimethyl derivative **3c** [1.652(4), 40.2(1)º],[25] which was prepared from **3b** upon treatment with BuLi followed by MeI (Scheme 7). It holds true for the di(spiroacridan) analogues **8b**,**c** with the two bay-region substituents, which exhibit similar structural parameters [**8b**: 1.651(6) Å, 38.7(1)º; **8c**: 1.649(3) Å 39.2(2)º],[32] showing that the 9,10-dihydrophenantherene-type HPEs with two spiro(tricyclic system) at 9,10-positions adopt the similar strained molecular structure as inherited from HPE.

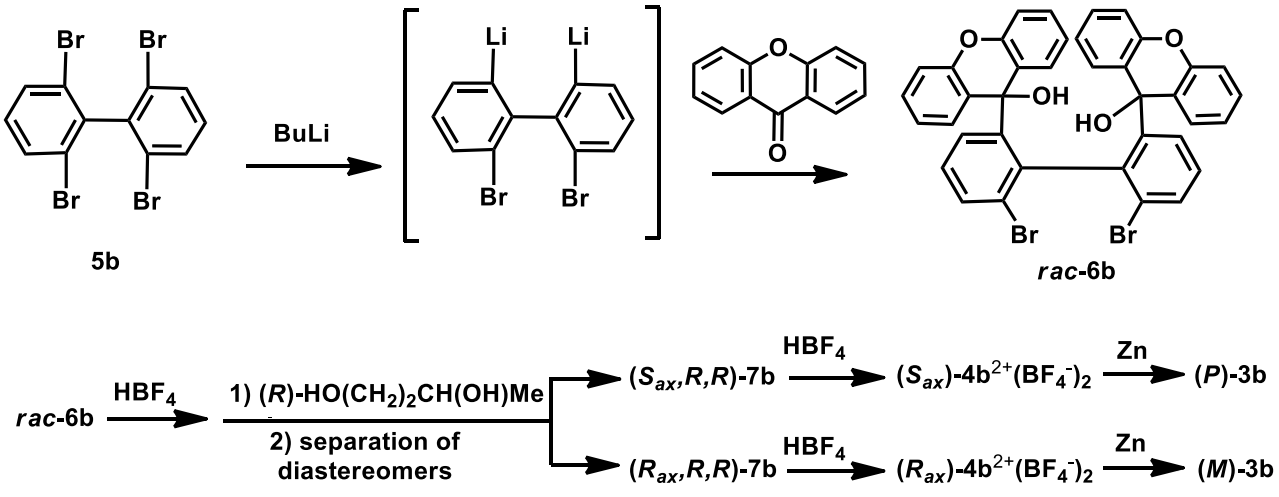

Scheme 6

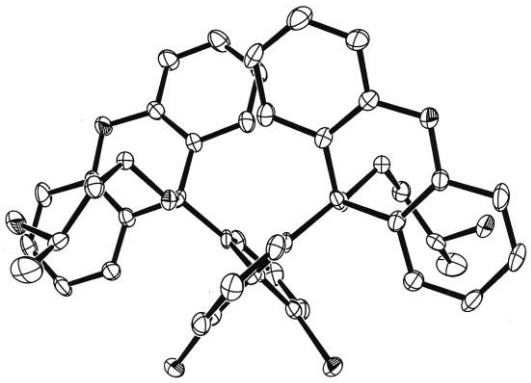

Figure 8. X-Ray structure of (R_{ax},*R*,*R*)-**7b**

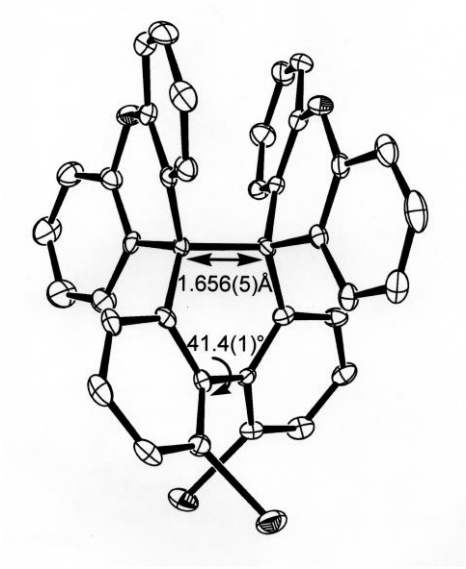

Figure 9. X-Ray structure of **3b**

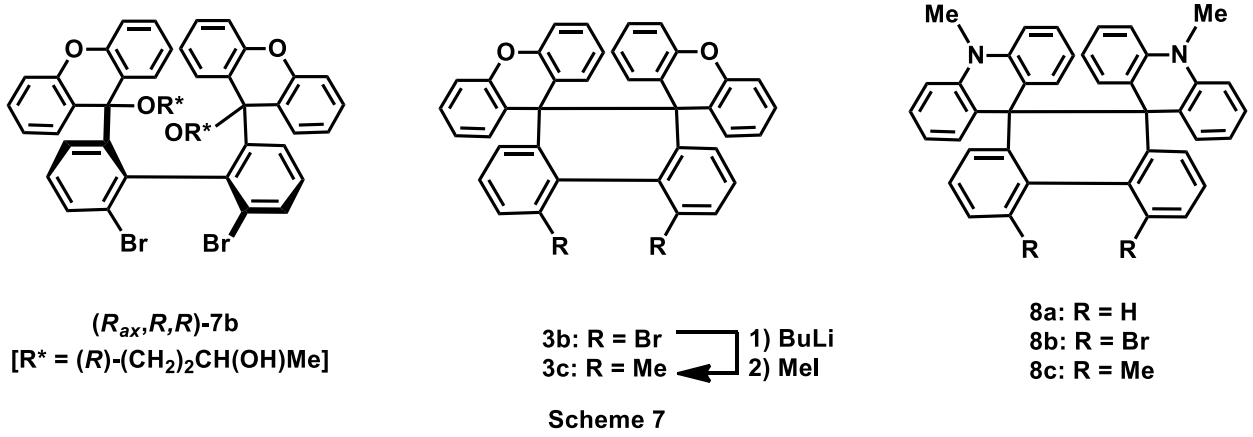

Scheme 7

The helically twisted structure is favorable to attain strong exciton coupling of two chromophores arranged in the asymmetric manner to induce the large Cotton effects. As shown in Figure 10, (*M*)/(*P*)-**3b** and (R_{ax})/(S_{ax})-**4b**$^{2+}$ show strong bisignated Cotton effects in the UV and visible region, respectively. Such large Cotton effects allowed us to observe a drastic CD spectral change accompanied by electrochromism upon electrolysis (Figure 11). The spectral changes with several isosbestic points indicated clean conversion as well as negligible steady-state concentration of the intermediary cation radical thanks to the dyrex behavior (Table 1) with one-wave 2e-transfer. This is the successful example of electrochiroptical response systems in the early stage of their studies. Thereafter, the above molecular design concept has been used to construct a series of advanced electrochiroptical systems, such as **8b** and **8c**.[32b]

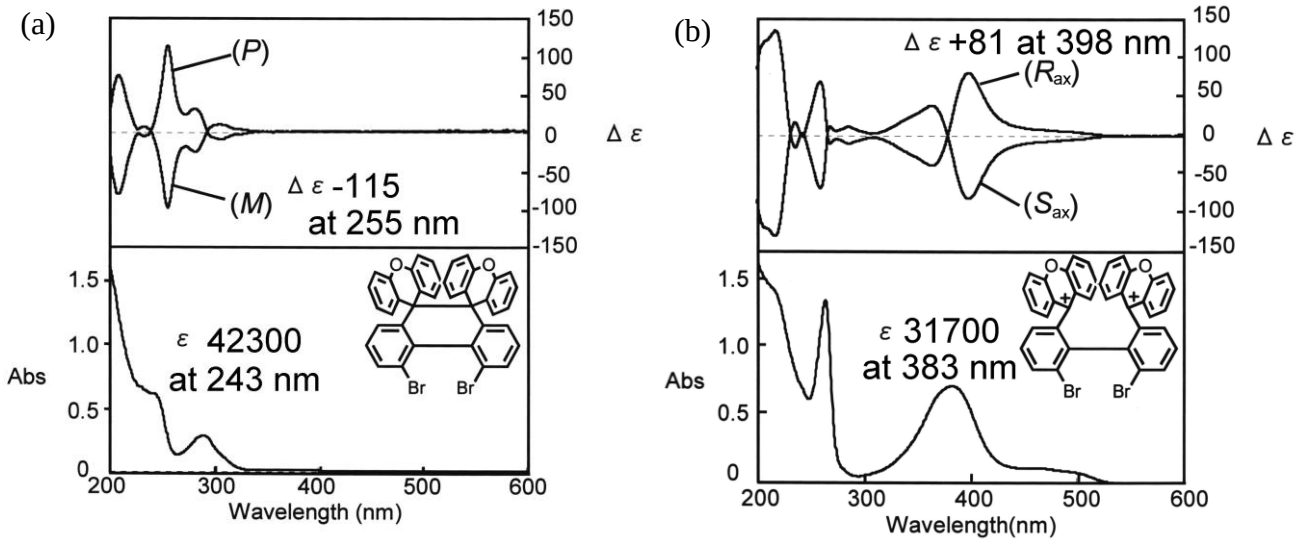

Figure 10. (upper) CD and (lower) UV-Vis spectra of optically pure (a) **3b** and (b) **4b**$^{2+}$(BF_4^-)$_2$ measured in MeCN

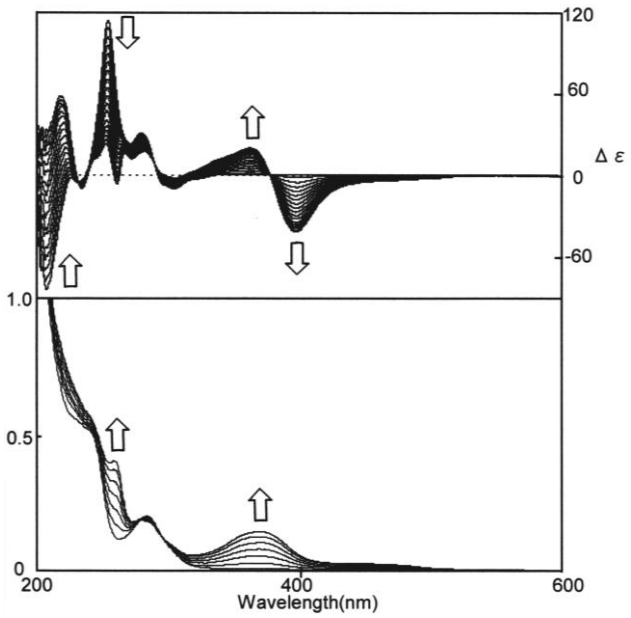

Figure 11. (upper) CD and (lower) UV-Vis spectral changes of optically pure (*P*)-**3b** upon constant-current electrochemical oxidation in MeCN containing 0.05 M Bu_4NBF_4 as an electrolyte

Table 1. Redox potentials[a] of **3** and **4**$^{2+}$ measured in CH_2Cl_2

	E^{ox} of **3**	E^{red} of **4**$^{2+}$
3a/**4a**$^{2+}$	+1.30[b]	+0.46[b]
3b/**4b**$^{2+}$	+1.45[b]	+1.51[b]

[a] Peak potentials, *E*/V vs SCE, Pt electrode. [b] two-electron process.

3.2 Redox-induced fluorescence switching

Molecular switches for fluorescence have been attracting considerable attention, especially because of high sensitivity of luminescence signals. Redox-dependency of fluorescence has been mainly studied by using metal-centered redox couples, where the interaction between the redox-active site (transition metal complex) and the external fluorophore plays an important role for the ON/OFF mechanism.[33] Pure organic switches without metal ions are rare, and the first example was reported by using tetrathiafulvalene as a redox center and free-base porphyrin as a fluorophore.[34] We envisaged that new fluorescence switch could be realized by using dyrex pair of **1** and $\mathbf{2}^{2+}$ as the redox center with incorporating suitable fluorophore, such as phenanthrene, triphenylene, or dibenzoanthracene, as in **9a** - **9c**, which were prepared from dibromo derivative **3b** as shown in Scheme 8.[35]

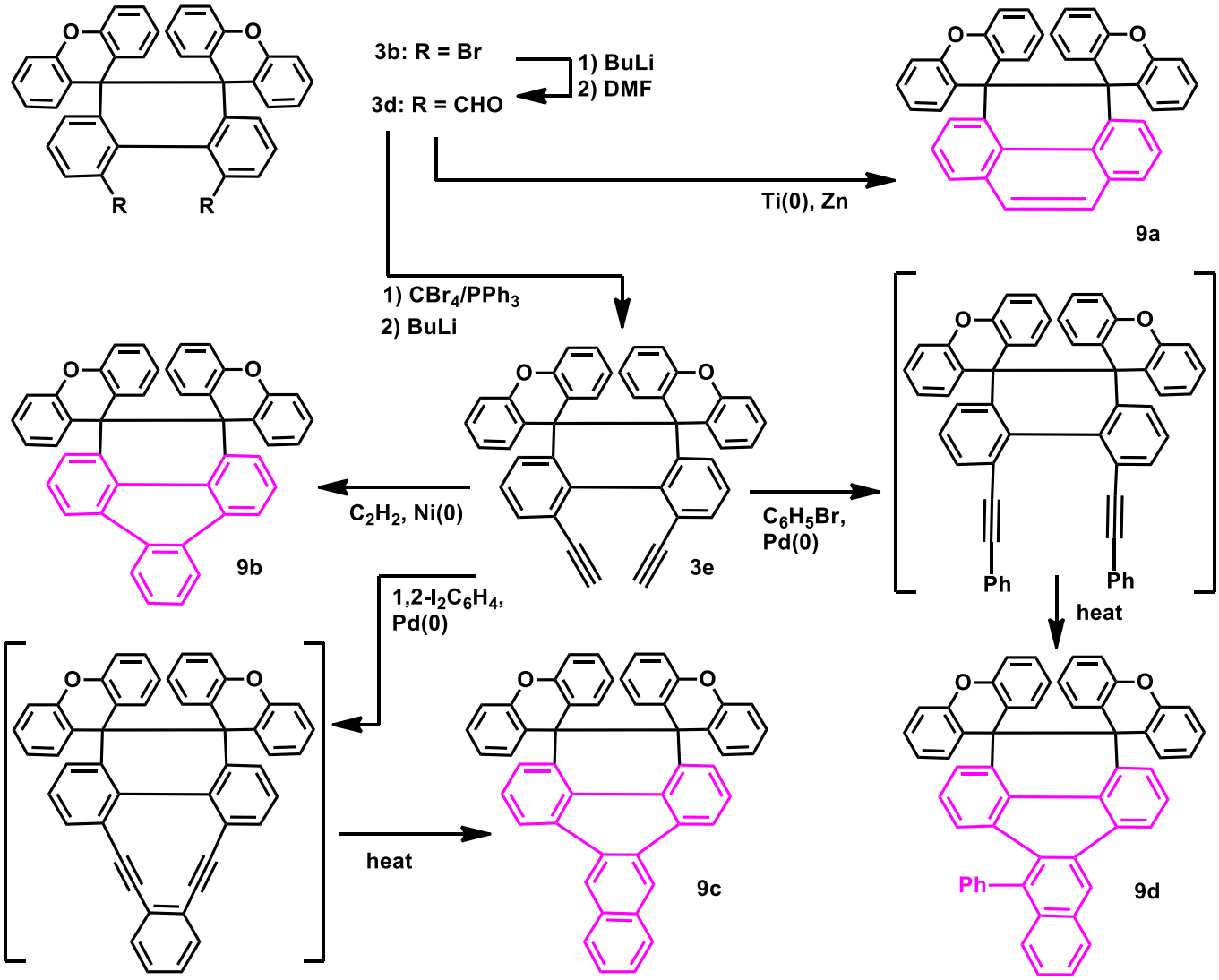

Scheme 8

Thus, dialdehyde **3d** was prepared upon treatment of **3b** with BuLi followed by DMF, which was subjected to the McMurry coupling reaction to give **9a**. By considering the reported difficulty to convert 2,2'-dihalobiphenyls to the corresponding diynes via Pd-catalyzed reactions,[36] diacetylene **3e** was prepared form **3d** via a bis(dibromomethylene) intermediate. Then, Ni(0)-catalyzed [2+2+2] co-cyclization[37] under the acetylene atmosphere gave **9b**. The Pd(0)-catalyzed Sonogashira coupling of **3e** with 1,2-diiodobenzene gave **9c** via spontaneous Masamune-Bergman cyclization[38] of the intermediary macrocycle. The dibenzoanthracene skeleton in **9c** was more easily constructed by the cyclization[39] of bis(phenylethynyl) derivative to give **9d**. A variety of reactions shown in Scheme 8 indicate that the dyrex skeleton of **1** is robust enough to various transformations, especially to the cross coupling conditions using transition metals, thus providing other dyrex skeletons[40] for post-transformation strategy.

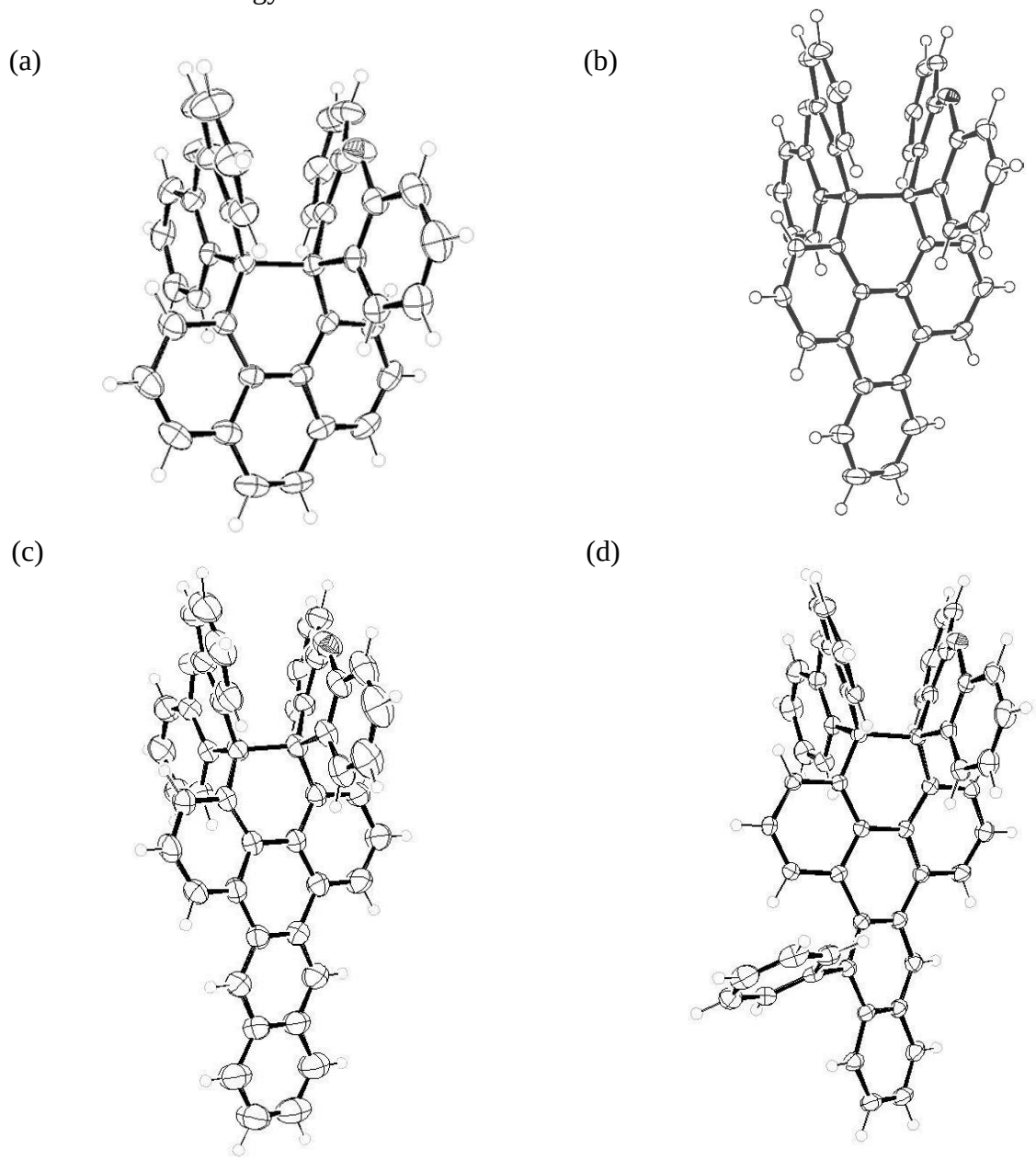

Figure 12. X-Ray structures of (a) **9a**, (b) **9b**, (c) **9c**, and (d) **9d** measured at 153 K

Their structural features were revealed by the X-ray analyses (Figure 12), and the C-C bond lengths corresponding to the "ethane" bond are summarized in Table 2. Although the values [*d*: 1.614(2) - 1.630(2) Å] are beyond the standard length due to HPE skeleton, slightly shorter values than those of **3b** or **3c** [1.656(5), 1.652(4) Å] are due to the condensation of a polyaromatic unit, that changes the skewing angle of the dihydrophenanthrene skeleton.[32a] Despite such structural constraint by the fused ring, all of **9a** - **9d** undergo 2e-oxidation (Table 2) to give the corresponding dications **10a**$^{2+}$ - **10d**$^{2+}$ (Scheme 9), which were isolated as stable $(SbCl_6^-)_2$ salts. We succeeded in analyzing the X-ray structure of **10a**$^{2+}$ salt. As expected, the two xanthenylium units are forced to overlap in a face-to-face manner with the very close C9$^+$ -- C9$^+$ contact of 3.06 Å (Figure 13), which is one of the shortest C$^+$ -- C$^+$ intramolecular distances between triarylmethyliums.[41]

Table 2. Bond length[a] and fluorescence quantum yield[b] of **9**, and redox potentials[b,c] of **9** and **10**$^{2+}$

	bond length (*d*)	Φ_f	E^{ox} of **9**	E^{red} of **10**$^{2+}$
9a/**10a**$^{2+}$	1.625(2) Å	0.01	+1.13[d]	+0.60[d]
9b/**10b**$^{2+}$	1.630(2) Å	0.01	+1.13[d]	+0.60[d]
9c/**10c**$^{2+}$	1.626(3) Å	0.07	+1.12[d]	+0.63[d]
9d/**10d**$^{2+}$	1.614(2) Å	0.02	+1.14[d]	+0.54[d]

[a] Determined by X-ray structural analyses at 153 K. [b]Measured in MeCN. [c] Peak potentials, *E*/V vs SCE, Pt electrode. [d]Two-electron process.

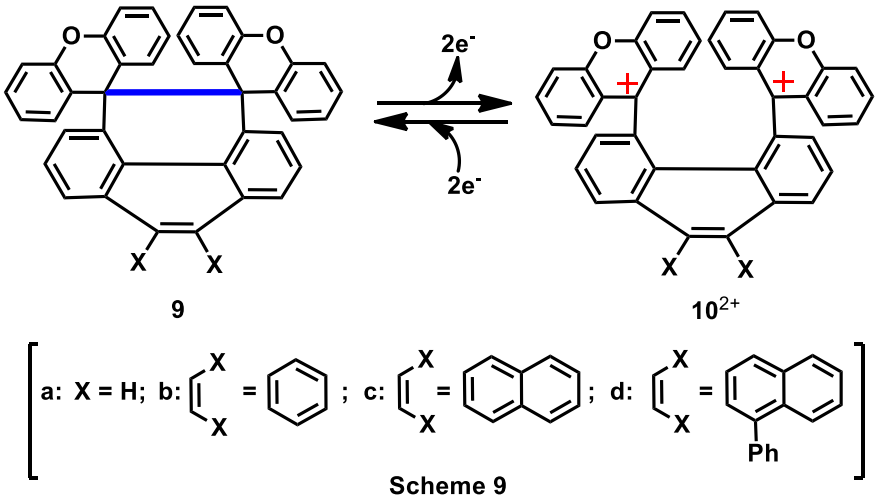

Scheme 9

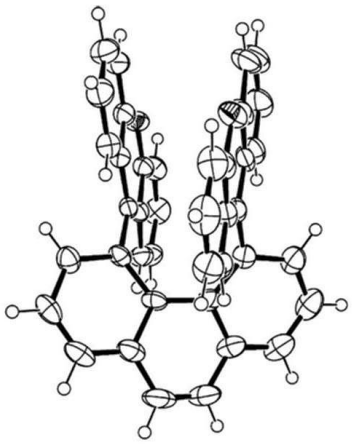

Figure 13. X-Ray structure of **10a**$^{2+}$ in **10a**$^{2+}(SbCl_6^-)_2$ salt

Although the fluorescence quantum yields of **9a** - **9d** are not high (Table 2), electrochemical oxidation induced not only UV-Vis spectral change but also steady decrease in fluorescence (Figure 14a) since the fluorescence is completely quenched in the corresponding dications **10a**$^{2+}$ - **10d**$^{2+}$. This is a successful demonstration of another category of multi-output response systems. As shown in Scheme 10a, the fluorescence of **9d** disappears upon 2e-oxidation to **10d**$^{2+}$. On the other hand, another switching pattern (Scheme 10b) would be possible, when 2e-oxidation induces fluorescence growth. Actually, the latter could be realized by modifying the chromophore of the prototype **1**/**2**$^{2+}$. Thus, thanks to the fluorescent nature of acridinium skeleton, di(spiroacridan)-type HPE **8a** exhibits redox-induced fluorescence switching with steady increase of emission upon 2e-oxidation (Figure 14b).[20,42]

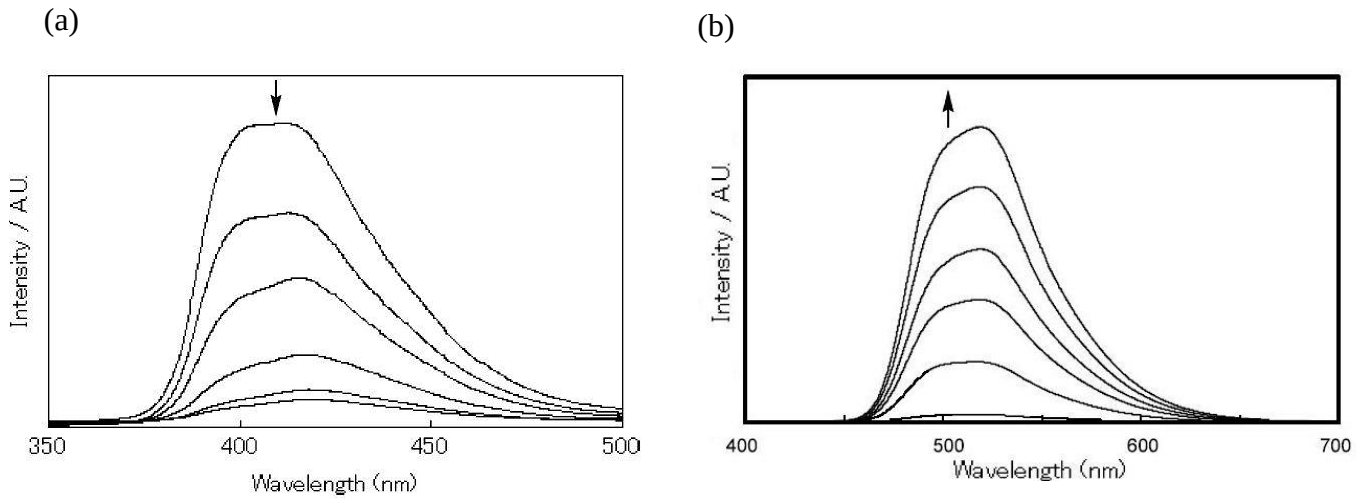

Figure 14. A fluorescence spectral change of (a) **9d** and (b) **8a** upon constant-current electrochemical oxidation in MeCN containing 0.05 M Et_4NClO_4 as an electrolyte

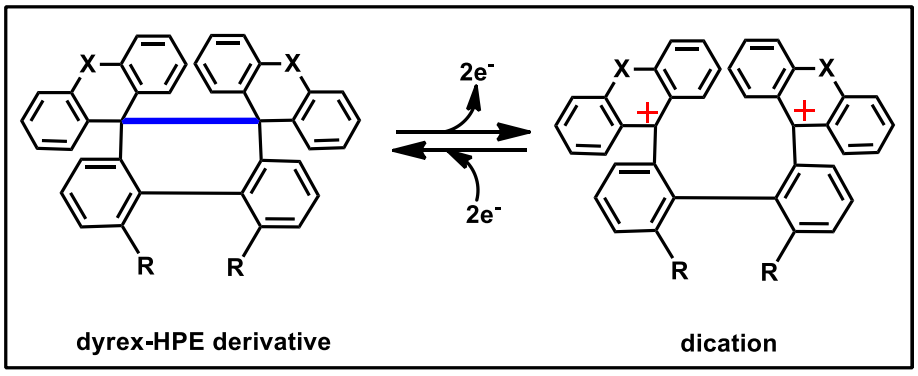

(a) FLUORESCENT ····· non-fluorescent [e.g. X = O, R-R = CH=CH, as in 9a]

(b) non-fluorescent ····· FLUORESCENT [e.g. X = N-Me, R = H, as in 8a]

Scheme 10

3.3 Multi-input-multi-output response system

In the field of molecular electronics,[43] the multi-input response systems have been considered as "molecular logic gates"[44] since the two independent external stimuli affect the physical/spectral properties, so that the transduced signals can be considered as if the molecule works as a logic operator such as "AND", "NOT" or "OR".[45] We envisaged that, by some modifications of the prototype structure of **1**/**2**$^{2+}$, we could construct the multi-input systems, using pH or heat as another input signal in addition to the electric potential. Furthermore, multi-input-multi-output system could be possible by addition of chiroptical output signal to UV-Vis, which prompted us to investigate on the synthesis and characterization of 2,7-dihydroazepin-fused helical pair of **11**/**12**$^{2+}$.[46]

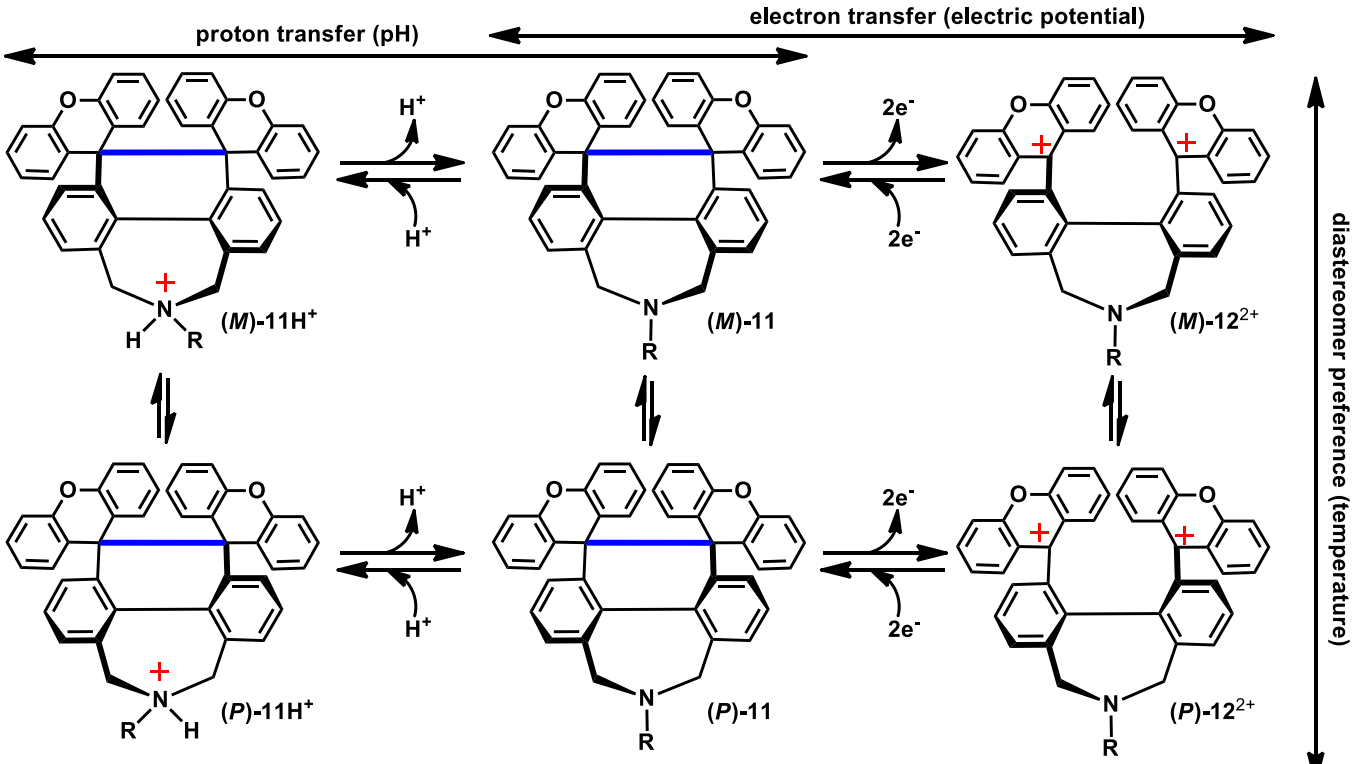

Scheme 11

As shown in Scheme 11, the bay-region carbons of the prototype (**1**/**2**$^{2+}$) are bridged with a CH_2-N(R)-CH_2 unit in the newly designed pair. Different from benzannulation as in **9**, this bridge is long enough to maintain the helical geometry of the biphenyl unit whereas the sp_3 N atom on the center can provide the pH-responsive function. When we attach a point chirality on the N atom, helical preference of the biphenyl unit would be induced by the intramolecular chiral transmission.[47] Thus, the helically biased pair of **11**/**12**$^{2+}$ with a chiral center on N would be two-way (UV-Vis and CD) output response system, whose properties would be changed not only by electric potential but also by pH. Because the diastereomeric ratio through the intramolecular chiral transmission is the function of

temperature, chiroptical output would be also affected by temperature, thus the three-way-input and two-way-output response would be formulated.

Although the tetrahydrophenanthro[4,5-*cde*]azepine skeleton in **11** has been hitherto unknown skeleton, several derivatives with a difference substituent on N were readily obtained from the dialdehyde **3d** through the reactions with the corresponding amine to give the diimine intermediates, which were then subjected to reductive cyclization[48] by using DIBALH to furnish the desired electron donors **11a**-**11d** (Scheme 12). The ^{1}H NMR spectrum of benzyl derivative **11d** is that for C_{2v}-symmetric species at 298 K, showing the rapid ring-flip between two energy-equivalent helical structures of the phenanthrazepine skeleton (Scheme 11). Upon lowering the measurement temperature, the broad signal for the methylene protons were finally separated into two (3.55 and 3.93 ppm in $CDCl_3$), which were assigned to the diastereomeric protons of the helically deformed seven-membered ring. Based on the VT-NMR analysis, the inversion barrier of 13.9 kcal mol^{-1} was determined for **11d**.

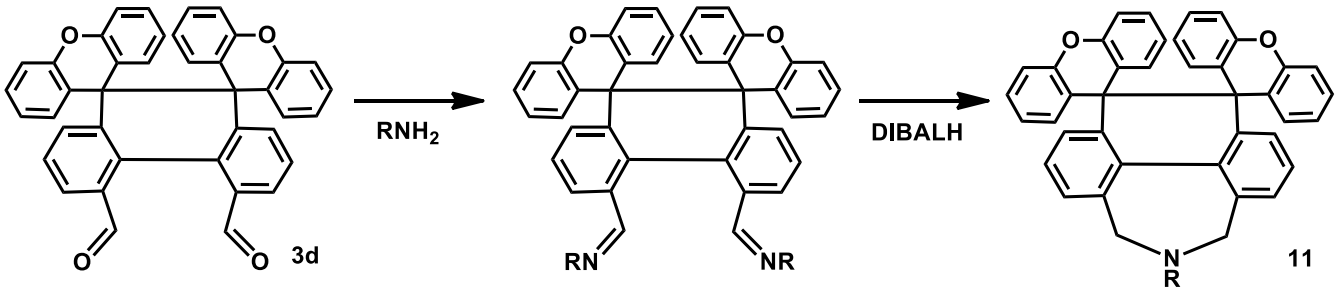

[a: R = (*R*)-PhCHMe; *ent*-a: R = (*S*)-PhCHMe; b: R = (*R*)-cHexCHMe; c: R = (*R*)-4-FC_6H_4CHMe; d: R = $PhCH_2$]

Scheme 12

For **11a** - **11c** with an asymmetric center on N, interconversion of diastereomers is also suppressed at low temperature to give two sets of ^{1}H NMR resonances, from which the diastereomeric ratios were determined (75:25 for **11a**; 55:45 for **11b**; 82:18 for **11c** at 213K in $CDCl_3$). These ratios correspond to the degree of intermolecular asymmetric transmission from the point chirality on N to the helicity of phenanthrazepine skeleton, which is effective by the aromatic auxiliary in **11a** but not by the aliphatic counter part (**11b**). Crystallization of **11a** gave a single crystal containing only (*M*)-isomer whereas the crystal lattice of **11b** contains both diastereomers in a 1:1 ratio (Figure 15), which is in accord with the degree of diastereomeric preference in solution. Slightly higher diastereomeric ratio was attained by the electron-withdrawing aryl group (**11c**) than in **11a**, suggesting that chiral auxiliary is close to the biphenyl unit in solution, and π - π interaction[49] but not C-H -- π interaction[50] is more important to attain the observed diastereomeric preference by the aromatic auxiliary.

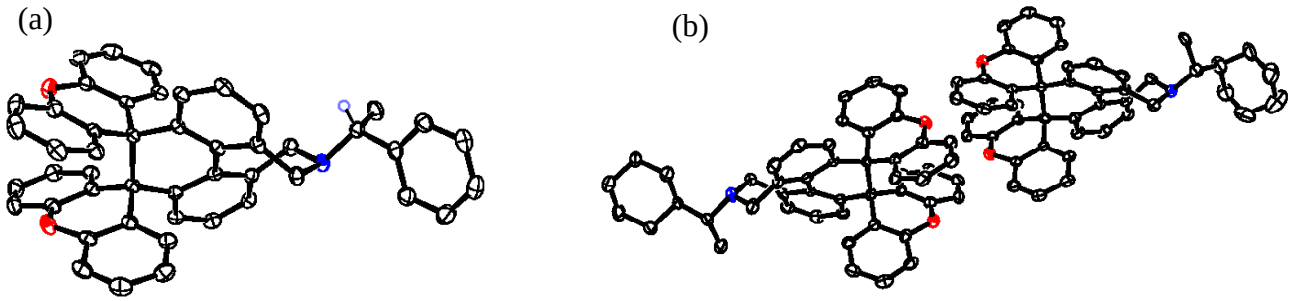

Figure 15. (a) X-Ray structure of **11a** attached with (*R*)-PhCHMeN group. The crystal contains only (*M*)-isomer (100% de). (b) X-Ray structure of **11b** attached with (*R*)-cHexCHMeN group. The crystal contains both (*M*)- and (*P*)-isomers in 1:1 ratio (0% de).

Upon 2e-oxidation, the corresponding dications **12a**$^{2+}$- **12d**$^{2+}$ were isolated as stable salts. As shown by the strong CD couplet in the spectrum of **12a**$^{2+}$, the point chirality of (*R*)-PhCHMeN induces significant helicity preference (Δε +33 at 401 nm, –25 at 371 nm in MeCN at 293 K), for which (*M*)-helicity is assigned by comparing the spectral shape with that of dibromo dication [(R_{ax})-**4b**$^{2+}$: Δε +81 at 398 nm, –39 at 366 nm]. As expected, *ent*-**11a** and *ent*-**12a**$^{2+}$ with an (*S*)-PhCHMeN auxiliary exhibit the CD signals of mirror-image (Figure 16). By considering that the simple asymmetric center induces a very small Cotton effect (Δε < 5),[29] intramolecular chiral transmission to the helicity is proven the effective protocol to amplify the Cotton effects.[51] The large Cotton effects both in **11a** and **12a**$^{2+}$ as well as the wavelength shift from UV (**11a**) to visible region (**12a**$^{2+}$) enable this dyrex pair to serve as electrochiroptical response system.

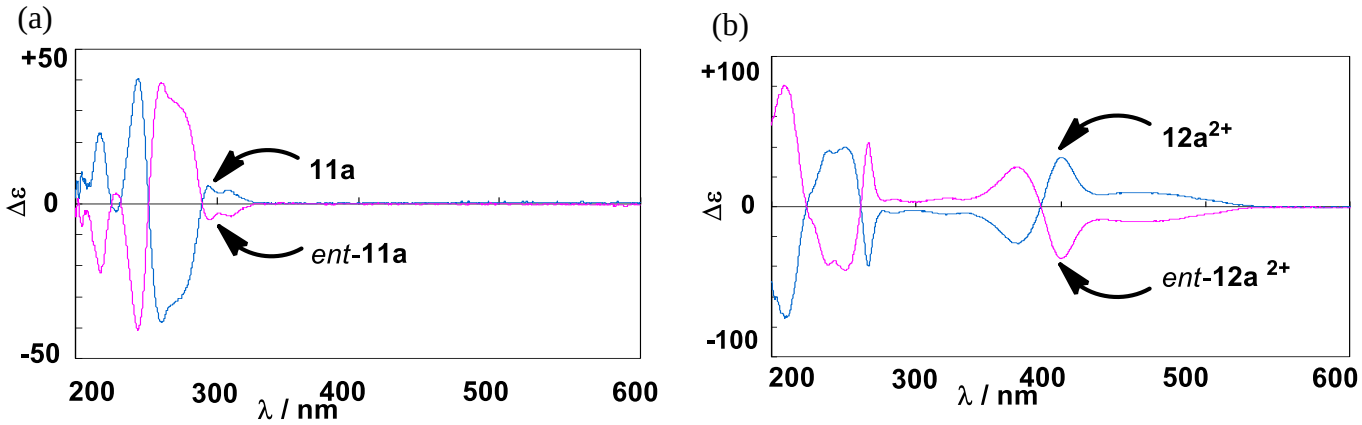

Figure 16. CD spectra of (a) **11a** and *ent*-**11a**, and (b) those of **12a**$^{2+}$($SbCl_6^-$)$_2$ and *ent*-**12a**$^{2+}$($SbCl_6^-$)$_2$ measured in MeCN at 293 K

On the other hand, more prominent feature of **11a**/**12a**$^{2+}$ is the multi-input function to modify the chiroptical properties by heat and pH. Thus, the diastereomeric ratio changes by the temperature. The increase in CD spectral intensity was observed both in the spectra of **11a** and **12a**$^{2+}$ upon lowering the measurement temperature from 293 K to 243 K (Figure 17). Furthermore, protonation on N by addition of TsOH to an MeCN solution of **11a** caused dynamic changes in both of UV and CD spectra (Figure 18). This is the successful demonstration of three-way-input-and-two-way-output molecular response system, which initiated the related studies on other dyrex systems by incorporating fluorescence and fluorescence-detected CD spectra as additional outputs.[19,52]

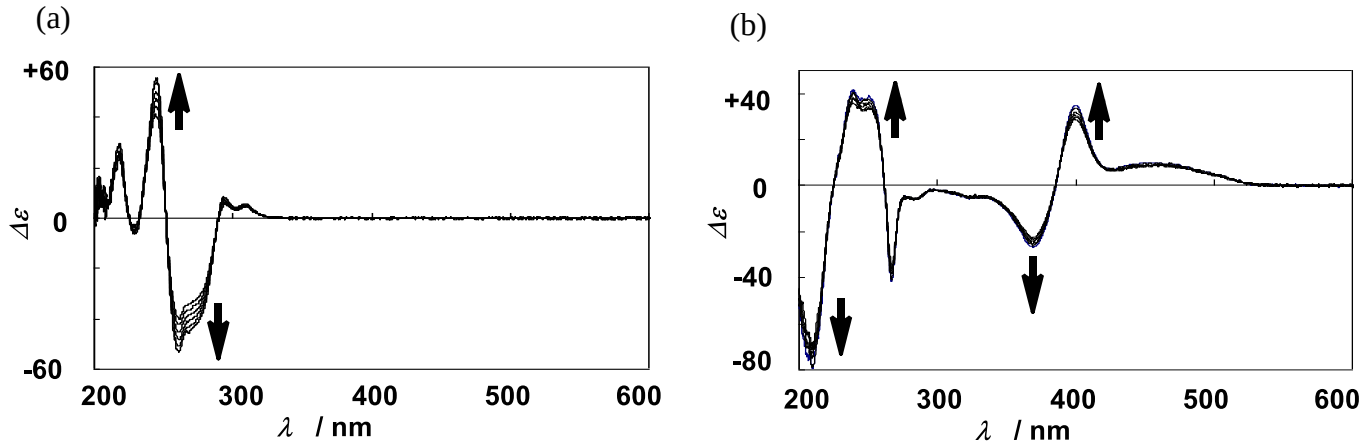

Figure 17. Continuous changes in CD spectra upon changing the solution temperature of (a) **11a** and (b) **12a**$^{2+}$$(SbCl_6^-)_2$ from 293 K to 243 K in MeCN

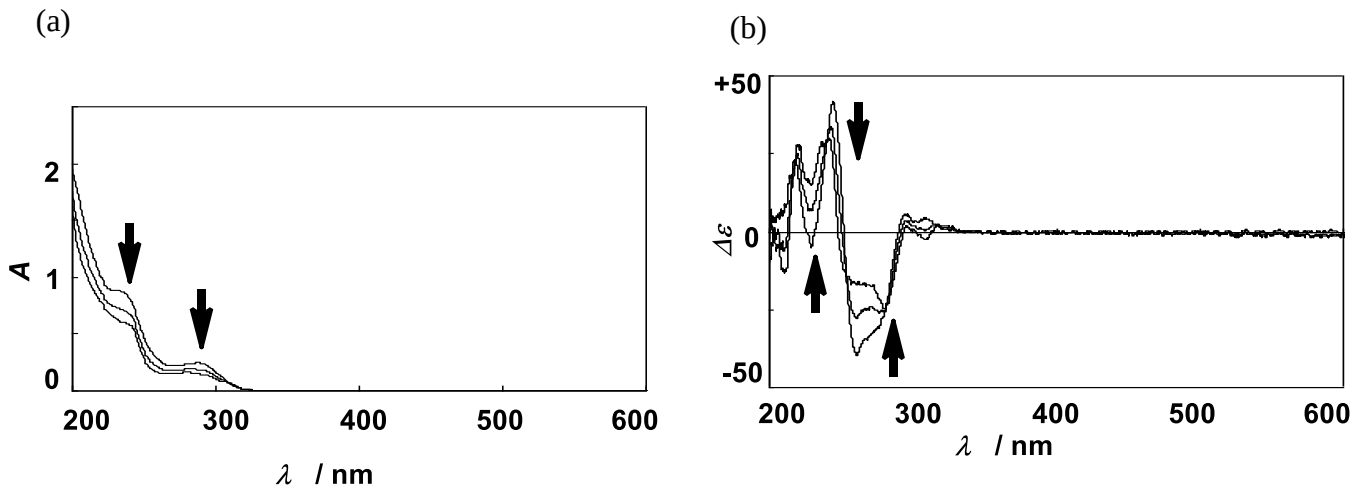

Figure 18. (a) UV and (b) CD spectral changes of **11a** upon the addition of 0.5 and 1 equivalent of TsOH in MeCN at 293 K

4. Further structural modification for more advanced functions

4.1 Toward chiral redox memory

The helical inversion in **11**/**12**$^{2+}$ is the key for the intramolecular transmission of point chirality to induce the preference of helical sense of the molecular framework. When the helicity preference is induced by the *inter*molecular manner[53] in the further structurally modified prototype of **1**/**2**$^{2+}$, such a chirality transfer from external asymmetric source would furnish the unique functions such as chiral memory[54] or chiral amplification.[55] For the transfer of external chirality ("writing" process), inversion of helicity should occur very easily. On the other hand, inversion of helicity should be prevented by a certain chemical transformation to maintain the induced chirality ("memorizing" process). Transformation should be reversible to allow helical inversion to erase the induced chirality ("erasing" process), and thus electrochemical transformation would be useful to construct the chiral redox memory based on the dyrex systems.

By considering the larger inversion barrier of **2**$^{2+}$ than **1**, we envisaged that, under proper molecular design (e.g. **13**/**14**$^{2+}$),[56] neutral species can undergo rapid helical inversion whereas the corresponding dication is configurationally stable to maintain its chiral information (Scheme 13). It should be noted that, thanks to the electrochemical bistability of the dyrex systems, the electron exchange between the neutral state ("writable/erasable" species) and dicationic state ("memorable" species) is prohibited, which

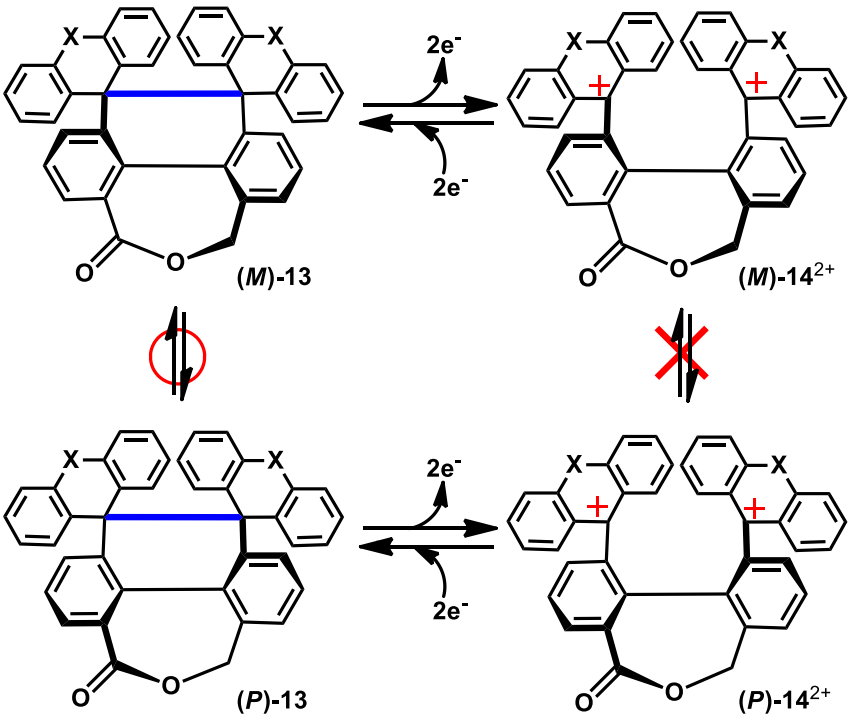

Scheme 13 [a: X = O; b: X = NMe]

is the essential requirement for the redox-type memories.[57] For the conventional redox systems undergoing reversible interconversion between the neutral and the charged species, memory effects could not be realized because of the facile electron exchange of the "memorable"-species with the "writeable/erasable"-species, thus losing the memorized information.

The CH_2-O-C(=O) bridge at the bay region of **13**/**14**$^{2+}$ has been selected after examining a series of compounds with different inversion barrier,[17,58] and 4,6,10,11-tetrahydrophenanthro[4,5-*cde*]oxepin-4-one **13a** with two siproxanthene units was designed. By the Tishchenko reaction[59] of dialdehyde **3d**, **13a** was obtained which undergoes two-electron interconversion with **14a**$^{2+}$($SbCl_6^-$)$_2$ salt. Bis(acridinium) analogue **14b**$^{2+}$ was obtained from another dialdehyde **15**[58b] by the similar condensation reaction followed by *N*-methylation of the two acridine units in 5,7-dihydrodibenzo[*c*,*e*]oxepin-5-one **16** (Scheme 14). The precursor **16** adopts deeply skewed geometry to stabilize its helical configuration (Figure 19). Actually, helical inversion of **16** is prohibited under ambient conditions ($\Delta G^{\ddagger} > 25$ kcal mol^{-1}) to allow its optical resolution by chiral HPLC at room temperature, and the observed CD spectrum did not change over the days. The ^{1}H NMR spectra of **14a**,**b**$^{2+}$ did not change upon heating to 150 °C, and their configurational stability is in line with the high inversion barrier of **16**. On the other hand, the ^{1}H NMR spectra of neutral donors **13a**,**b** correspond to those of C_2-symmetric species only at low temperature, and the VT-NMR analyses gave the values of $\Delta G^{\ddagger}$ of 16 kcal mol^{-1} for both **13a**,**b**.

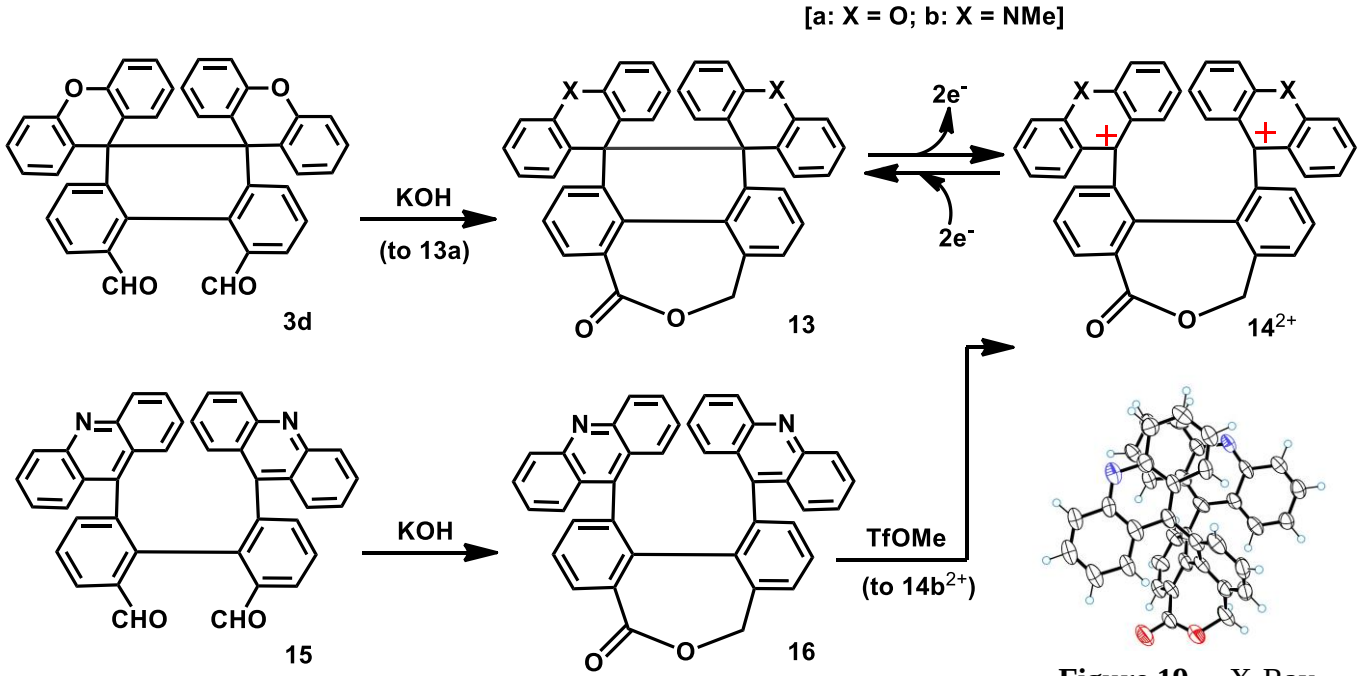

Scheme 14

Figure 19. X-Ray structure of **16**

In this way, we have succeeded in constructing the dyrex pairs of **13a/14a**$^{2+}$ (X = O) and **13b/14b**$^{2+}$(X = NMe), in which the dicationic state has a very large inversion barrier whereas the neutral state exhibits rapid ring-flip irrespective to the kind of heterocycles (xanthene/acridan) as the electrophore units. As shown in the UV-Vis spectral changes upon electrolyses of **13a** and **13b**, their electrochromic behaviors from colorless to yellow-orange are also similar (Figure 20). On the other hand, the redox potentials are rather different between these pairs [E^{ox}/E^{red} vs SCE in MeCN: +1.11 V/+0.49 V for **13a/14a**$^{2+}$ and +0.30 V/–0.10 V for **13b/14b**$^{2+}$, respectively], so that the same approach is valid to construct the systems with the tunable working voltage by changing the heteroatom in the electrophore units.

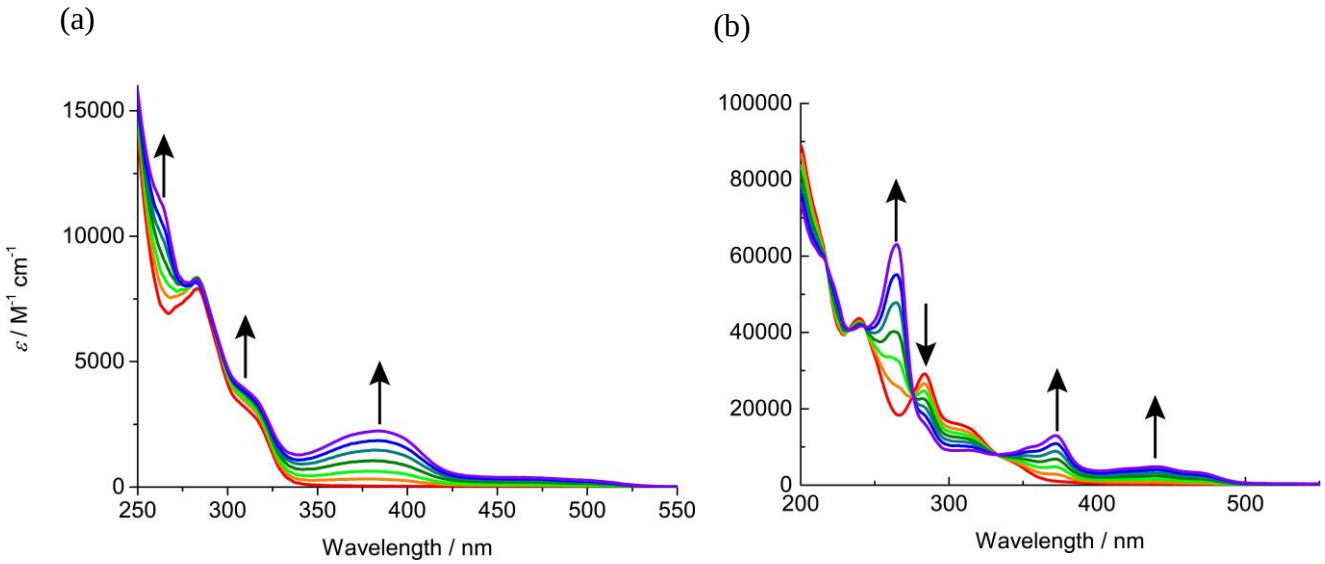

Figure 20. UV-Vis spectral change of (a) **13a** and (b) **13b** upon constant-current electrochemical oxidation in MeCN containing 0.05 M Et_4NClO_4 as an electrolyte

4.2 Redox-induced O_2-storage

As detailed in Section 1, the C-C bond formation of 9-phenylxanthenyl moiety is facilitated by spatial proximity of two radical centers upon reduction of **2**$^{2+}$ to form **1**. When another spacer is replaced for the biphenyl-2,2'-diyl in **2**$^{2+}$ so that the two radicals are more separated apart, the resulting C-C bond would be much longer and very weak,[60] and thus, other products[61] would be formed instead of HPE derivative. Actually, formation of bis(9-phenylxanthenyl)peroxide[62] was reported to be the end product of **II**,[6] and such formation of peroxides is a typical side reaction upon attempted generation of HPEs.[7]

When the resulting peroxide undergoes extrusion of O_2 accompanied by reformation of the starting dication, the redox-induced O_2-uptake/release could be realized, which can be considered as novel O_2-storage system. This is the case of 3,9-dihydrodibenzo[*c*,*f*][1,2,6]trioxonin **15a** with two

spiro(xanthene) units obtained upon 2e-reduction of diphenyl ether-2,2'-diyl dication **16a**$^{2+}$ (Scheme 15).[63] Although only a small numbers of 9-membered cyclic peroxides have been reported,[64] this medium-sized endoperoxide **15a** was isolated in 80% yield upon reduction of **16a**$^{2+}$ in aerated THF. The X-ray analysis showed that the O-O bond is expanded to 1.507(4) Å (Figure 21), however, not O-O bond but neighboring C-O bonds were cleaved upon 2e-oxidation, thus undergoing "oxidative deoxygenation" reaction. Actually, upon treating **15a** with $(2,4\text{-}Br_2C_6H_3)_3N^{+\bullet}SbCl_6^-$ (2 equiv.), **16a**$^{2+}(SbCl_6^-)_2$ was obtained in 99% yield along with evolution of O_2 gas (96% of calculated amount).

Similar behavior is observed for other pairs of **15b**/**16b**$^{2+}$ with thioxanthene units (X: O ->S)[63] or of **15c**/**16c**$^{2+}$ with diphenylsulfide unit (Y: O -> S),[65] thus allowing some structural/electronic variations. On the other hand, diphenyl ether-2,2'-diylbis(diarylmethylium)s (Ar = 4-$MeOC_6H_4$, 4-$Me_2NC_6H_4$[66]) did not undergo facile formation of endoperoxides, showing that the xanthene-type tricyclic skeletons are suitable for construction of redox-induced O_2-storage systems.[67]

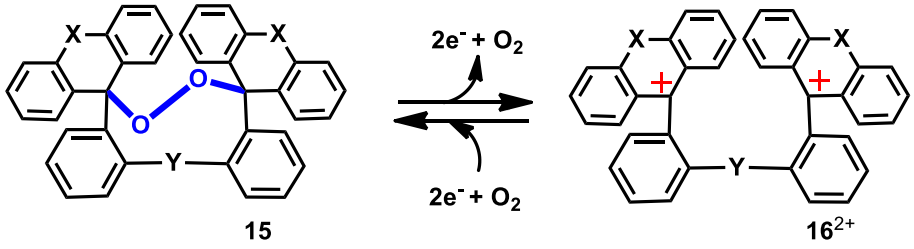

Scheme 15 **[a: X = Y = O; b: X = S, Y = O; c: X = O, Y = S]**

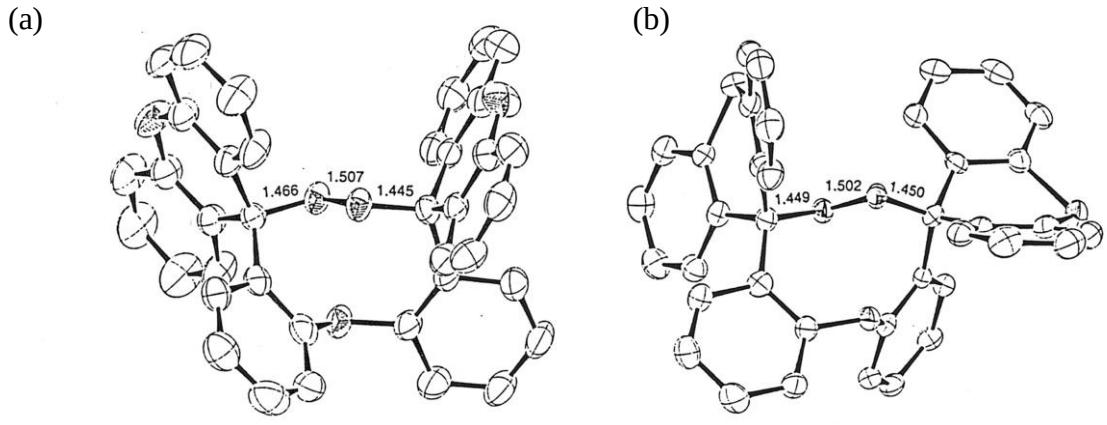

Figure 21. X-Ray structures of (a) **15a** and (b) **15b** (0.5AcOEt solvate). Both compounds have an extended conformation of the peroxide moiety [tortion angle: 160.8(3)° for **15a** and 154.6(2)° for **15b**, respectively].

5 Outlook

This review account describes the novel electrochromic systems based on the interconvertible dyrex pair of colorless HPE **1** and yellow-orange dication $\mathbf{2}^{2+}$, which can serve as a versatile scaffold to develop advanced molecular response systems. The electrochiroptical response systems ($\mathbf{3}/\mathbf{4}^{2+}$) and redox switches for fluorescence ($\mathbf{9}/\mathbf{10}^{2+}$) are multi-output response systems. Just by condensation with polyaromatic ring, fluorescent nature is induced in HPE skeleton whereas benzannulation or bromo substitution at the bay region can endow the electrochiroptical response. Helical geometries of $\mathbf{1}/\mathbf{2}^{2+}$ are also the key to conduct intramolecular chiral transmission to amplify the chiroptical properties in $\mathbf{11}/\mathbf{12}^{2+}$, and the temperature dependence of helicity preference enables to demonstrate multi-input response of CD spectrum. Furthermore, subtle change of the congesting degree at the bay region can control the energy barrier of helical inversion, and thus only the neutral HPE **13** but not the corresponding dication $\mathbf{14}^{2+}$ undergo ring-flip at ambient conditions to serve as the prototype of a chiral redox memory. All the above mentioned examples demonstrate that the prototype of $\mathbf{1}/\mathbf{2}^{2+}$ is one of the best scaffolds to develop the materials by following MFMS (maximum functions on the minimum skeleton)[20c] approach because only a small structural alternation can add new properties to the prototype, that can be used to exhibit new function.

Besides the facile structural modification of $\mathbf{1}/\mathbf{2}^{2+}$, tricyclic xanthene unit can find a way to tune its electronic nature by replacing the heteroatom. The red- and blue-shift of absorption is induced by replacing the heteroatom from O (xanthenylium) to S (thioxanthenylium) or NR (acridinium), respectively, whereas only acridinium emits strong fluorescence among three. Reduction potentials of O (xanthenylium) and S (thioxanthenylium) are much higher than that of NR (acridinium), so that the working potential of redox response can be also tunable on demand.

Finally, we like to point out another class of dyrex systems based on the same chromophores. Thus, the dyrex systems undergoing reversible intramolecular C-C bond formation/cleavage can be divided into two categories, endo-type and exo-type (Scheme 16),[20] and all of the dyrex systems shown in this article belong to the former since the positive charges are located on the endocyclic carbon of the ring undergoing C-C bond cleavage. In the latter category, the positive charges are located on the exocyclic carbon after the ring formation, as exemplified by $\mathbf{17}/\mathbf{18}^{2+}$ shown in Scheme 17.[68] They are structurally related to the pair of $\mathbf{3a}/\mathbf{4a}^{2+}$ with binaphthyl skeleton that connects two xanthene units. Upon 2e-oxidation, neutral donor **17** undergoes C-C bond formation to give $\mathbf{18}^{2+}$, and the xanthenylium units with positive charge are on the exocyclic bond. Upon reduction, the C-C bond in $\mathbf{18}^{2+}$ can be cleaved to regenerate diolefinic donor **17**. Reversible interconversion of $\mathbf{18}^{2+}$ with ether **19** under acidic/basic

conditions is applicable for multi-input protocol whereas three-way spectral outputs of UV-Vis, CD, and fluorescence detection are available during the interconversion. Although only a limited number of examples has been detailed in this article, the dyrex systems based on the xanthene-type and related chromophores seem to have an unlimited variation of molecular structures to develop the plethora of functional materials based on their unique electrochromic behaviors.

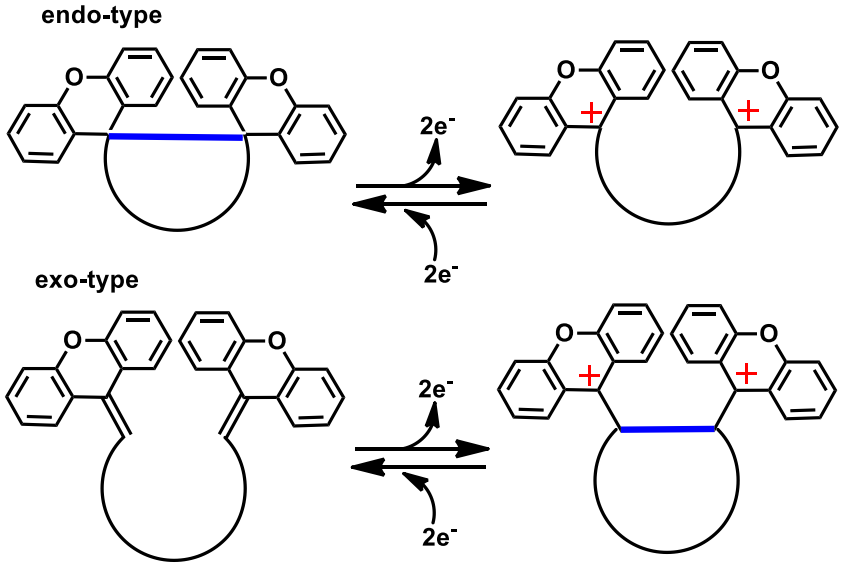

Scheme 16

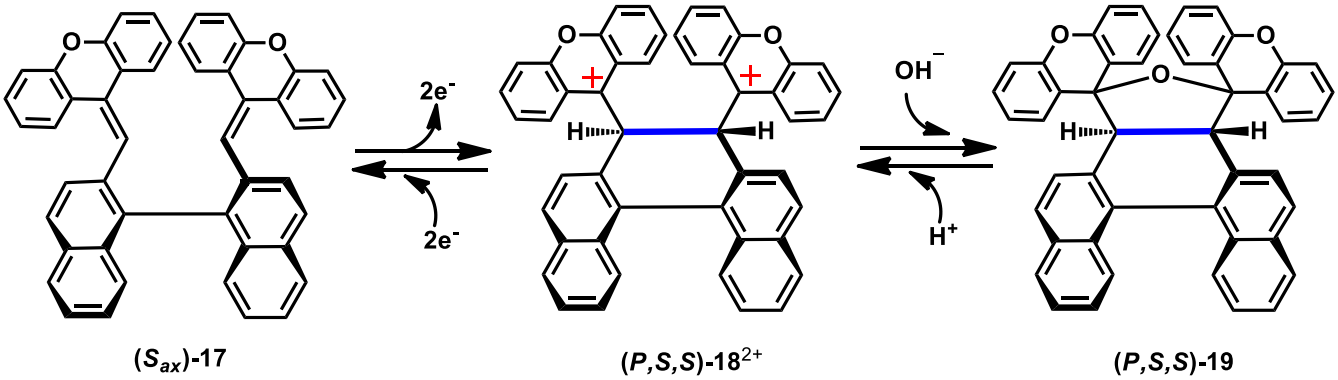

(S_{ax})-17 (P,S,S)-18^{2+} (P,S,S)-19

Scheme 17

ACKNOWLEDGEMENTS

We thank Grant-in-Aid from MEXT and JSPS (Nos. 18H04376, 19K15528, 20H02719, 20K21184) Japan. T.S. acknowledges The Orange Foundation for Hepatitis B Suit Hokkaido. Y.I. acknowledges Toyota Riken Scholar and The NOVARTIS Foundation (Japan) for the Promotion of Science. This work was also supported by the Research Program of "Five-star Alliance" in "NJRC Mater. & Dev." MEXT. Special thanks are due to Ms. Shoko Tanaka-Yamamoto for her great contribution for the studies shown in this review account.

REFERENCES AND NOTES

1. J. Loerke and F. Marlow, *Adv. Mater*., 2002, **14**, 1745.
2. (a) V. P. S. Perera, P. K. D. D. P. Pitigala, M. K. I. Senevirathne, and K. Tennakone, *Sol. Energy Mater. Sol. Cells*, 2005, **85**, 91; (b) P. K. Baviskar, J. B. Zhang, V. Gupta, S. Chand, and B. R Sankapal, *J. Alloys Compd.*, 2012, **510**, 33; (c) Y. -Q. Zhang, D. -K. Ma, Y. -G. Zhang, W. Chen, and S. -M. Huang, *Nano Energy*, 2013, **2**, 545.
3. M. Gomberg and L. H. Cone, *Justus Liebigs Ann. Chem.*, 1909, **370**, 142.
4. (a) E. M. Arnett, R. A. Flowers, A. E. Meekhof, and L. Miller, *J. Am. Chem. Soc*., 1993, **115**, 12603; (b) R. C. Gostowski, T. Bailey, S. D. Bonner, E. E. Emrich, and S. L. Steelman, *J. Phys. Org. Chem.*, 2000, **13**, 735.
5. T. Erabi, M. Asahara, M. Miyamoto, K. Goto, and M. Wada, *Bull. Chem. Soc. Jpn.*, 2002, **75**, 1325.
6. D. T. Hogan and T. C. Sutherland, *J. Phys. Chem. Lett.*, 2018, **9**, 2825.
7. J. M. McBride, *Tetrahedron*, 1974, **30**, 2009.
8. B. Kahr, D. Van Engen, and K. Mislow, *J. Am. Chem. Soc.*, 1986, **108**, 8305.
9. (a) S. Grimme and P. R. Schreiner, *Angew. Chem. Int. Ed.*, 2011, **50**, 12639; (b) S. Rösel, C Balestrieri, and P. R. Schreiner, *Chem. Sci.*, 2017, **8**, 405.
10. DFT calculations on III, **1** and $\mathbf{2}^{+}$ were conducted at B3LYP/6-31G(d) level: M. J. Frisch, G. W. Trucks, H. B. Schlegel, G. E. Scuseria, M. A. Robb, J. R. Cheeseman, G. Scalmani, V. Barone, G. A. Petersson, H. Nakatsuji, X. Li, M. Caricato, A. V. Marenich, J. Bloino, B. G. Janesko, R. Gomperts, B. Mennucci, H. P. Hratchian, J. V. Ortiz, A. F. Izmaylov, J. L. Sonnenberg, D. Williams-Young, F. Ding, F. Lipparini, F. Egidi, J. Goings, B. Peng, A. Petrone, T. Henderson, D. Ranasinghe, V. G. Zakrzewski, J. Gao, N. Rega, G. Zheng, W. Liang, M. Hada, M. Ehara, K. Toyota, R. Fukuda, J. Hasegawa, M. Ishida, T. Nakajima, Y. Honda, O. Kitao, H. Nakai, T. Vreven, K. Throssell, J. A. Montgomery, Jr., J. E. Peralta, F. Ogliaro, M. J. Bearpark, J. J. Heyd, E. N. Brothers, K. N. Kudin, V. N. Staroverov, T. A. Keith, R. Kobayashi, J. Normand, K. Raghavachari, A. P. Rendell, J. C. Burant,

S. S. Iyengar, J. Tomasi, M. Cossi, J. M. Millam, M. Klene, C. Adamo, R. Cammi, J. W. Ochterski, R. L. Martin, K. Morokuma, O. Farkas, J. B. Foresman, and D. J. Fox, Gaussian 16, Revision A.03, Gaussian, Inc., Wallingford CT, 2016.

11. F. H. Allen, O. Kennard, D. G. Watson, L. Brammer, A. G. Orpen, and R. Taylor, *J. Chem. Soc.*, *Perkin Trans. 2*, 1987, S1.
12. Reviews: (a) T. Suzuki, T. Takeda, H. Kawai, and K. Fujiwara, *Pure Appl. Chem.*, 2008, **80**, 547; (b) T. Takada, Y. Uchimura, H. Kawai, R. Katoono, K. Fujiwara, and T. Suzuki, *Chem. Lett.*, 2013, **42**, 954.
13. (a) A. A. Zavitsas, *J. Phys. Chem. A*, 2003, **107**, 897; (b) D. Cho, Y. Ikabata, T. Yoshikawa, J. Y. Lee, and H. Nakai, *Bull. Chem. Soc. Jpn.*, 2015, **88**, 1636.
14. (a) P. R. Schreiner, L. V. Chernish, P. A. Gunchenko, E. Y. Tikhonchuk, H. Hausmann, M. Serafin, S. Schlecht, J. E. P. Dahl, R. M. K. Carlson, and A. A. Fokin, *Nature*, 2011, **477**, 308; (b) A. A. Fokin, L. V. Chernish, P. A. Gunchenko, E. Y. Tikhonchuk, H. Hausmann, M. Serafin., J. E. P. Dahl, R. M. K. Carlson, and P. R. Schreiner, *J. Am. Chem. Soc.*, 2012, **134**, 13641.
15. G. Wittig and H. Petri, *Justus Liebigs Ann. Chem.*, 1933, **505**, 17.
16. W. D. Hounshell, D. A. Dougherty, J. P. Hummel, and K. Mislow, *J. Am. Chem. Soc.*, 1977, **99**, 1916.
17 T. Suzuki, J. Nishida, and T. Tsuji, *Angew. Chem., Int. Ed. Engl.*, 1997, **36**, 1329.
18. (a) T. Suzuki, J. Nishida, and T. Tsuji, *Chem. Commun.*, 1998, 2193; (b) T. Suzuki, Y. Ishigaki, T. Iwai, H. Kawai, K. Fujiwara, H. Ikeda, Y. Kano, and K. Mizuno, *Chem. Eur. J.*, 2009, **15**, 9434; (c) Y. Ishigaki, T. Suzuki, J. Nishida, A. Nagaki, N. Takabayashi, H. Kawai, K. Fujiwara, and J. Yoshida, *Materials*, 2011, **4**, 1906.
19. (a) V. D. Parker, *J. Chem. Soc. D: Chem. Commun.*, 1969, 848; (b) D. H. Evans, *Chem. Rev.*, 1990, **90**, 739.
20. Reviews: (a) T. Suzuki, H. Higuchi, T. Tsuji, J. Nishida, Y. Yamashita, and T. Miyashi, In *Chemistry of Nanomolecular Systems, Chapter 1*, Springer-Verlag, Heidelberg, 2003; pp. 3-24; (b) T. Suzuki, E. Ohta, H. Kawai, K. Fujiwara, and T. Fukushima, *Synlett*, 2007, 851; (c) T. Suzuki, T. Takeda, E. Ohta, K. Wada, R. Katoono, H. Kawai, and K. Fujiwara, *Chem. Rec.*, 2015, **15**, 280; (d) T. Suzuki, H. Tamaoki, J. Nishida, H. Higuchi, T. Iwai, Y. Ishigaki, K. Hanada, R. Katoono, H. Kawai, K. Fujiwara, and T. Fukushima, In *Organic Redox Systems, Chapter 2*, Wiley, Hoboken, 2015, pp.13-37.
21. L. Pauling, In *The Nature of the Chemical Bond*, Cornell University Press, Ithaca, 1960.
22. R. Hoffman, *Acc. Chem. Res.*, 1971, **4**, 1.

23. Y. Ishigaki, Y. Hayashi, K. Sugawara, T. Shimajiri, W. Nojo, R. Katoono, and T. Suzuki, *Molecules*, 2017, **22**, 1900.
24. (a) P. Maslak, J. N. Narvaez, and T. M. Vollombroso, Jr., *J. Am. Chem. Soc.*, 1995, **117**, 12373; (b) P. Maslak, W. H. Chapman, Jr., and T. M. Vollombroso, Jr., *J. Am. Chem. Soc.*, 1995, **117**, 12380.
25. T. Suzuki, R. Yamamoto, H. Higuchi, E. Hirota, M. Ohkita, and T. Tsuji, *J. Chem. Soc., Perkin Trans. 2*, 2002, 1937.
26. T. Suzuki, J. Nishida, E. Hirota, M. Ohkita, and T. Tsuji, *Synth. Met.*, 2003, **133-134**, 357.
27. (a) C. Westermeier, H.-C. Gallmeier, M. Komma, and J. Daub, *Chem. Commun.*, 1999, 2427; (b) G. Beer, C. Niederalt, S. Grimme, and J. Daub, *Angew. Chem. Int. Ed*., 2000, **39**, 3252.
28. N. Berova, K. Nakanishi, and R. W. Woody, In *Circular Dichroism: Principles, Applications*, Wiley-VCH, New York, 2000.
29. (a) T. Mori and Y. Inoue, *J. Phys. Chem. A*, 2005, **109**, 2728; (b) T. Suzuki, T, Iwai, E. Ohta, H. Kawai, and K. Fujiwara, *Tetrahedron Lett.*, 2007, **48**, 3599.
30. J. Nishida, T. Suzuki, M. Ohkita, and T. Tsuji, *Angew. Chem. Int. Ed.*, 2001, **40**, 3251.
31. (a) R. H. Martin, M. Flammang-Barbieux, J. P. Cosyn, and M. Gelbcke, *Tetrahedron Lett.*, 1968, **9**, 3507; (b) D. H. Friese and G. Hättig, *Phys. Chem. Chem. Phys.*, 2014, **16**, 5942.
32. (a) K. Wada, T. Takeda, H. Kawai, R. Katoono, K. Fujiwara, and T. Suzuki, *Chem. Lett*., 2013, **42**, 1194; (b) T. Suzuki, Y. Kuroda, K. Wada, Y. Sakano, R. Katoono, K. Fujiwara, F. Kakiuchi, and T. Fukushima, *Chem. Lett*., 2014, **43**, 887.
33. Reviews: (a) R. Bergonzi, L. Fabbrizzi, M. Licchelli, and C. Mangano, *Coord. Chem. Rev*., 1998, **170**, 31; (b) L. Fabbrizzi, M. Licchelli, and P. Pallavicini, *Acc. Chem. Res*., 1999, **32**, 846; (c) A. Chevalier, P.-Y. Renard, and A. Romieu, *Chem. Asian J*., 2017, **12**, 2008
34. H. Li, J. O. Jeppesen, E. Levillain, and J. Becher, *Chem. Commun.*, 2003, 846.
35. T. Suzuki, S. Tanaka, H. Higuchi, H. Kawai, and K. Fujiwara, *Tetrahedron Lett.*, 2004, **45**, 8563.
36. M.-Y. Chou, A. B. Mandel, and M. -K. Leung, *J. Org. Chem*., 2002, **67**, 1505.
37. Y. Sato, T. Nishimata, and M. Mori, *J. Org. Chem*., 1994, **59**, 6133.
38. (a) N. Darby, C. U. Kim, J. A. Salaün, K. W. Shelton, S. Takada, and S. Masamune, *J. Chem. Soc., Chem. Commun.*, 1971, 1516; (b) R. G. Bergman, *Acc. Chem. Res*., 1973, **6**, 25.
39. (a) S. A. Kandil and R. E. Dessy, *J. Am. Chem. Soc.*, 1966, **88**, 3027; (b) E. H. White and A. A. F. Sieber, *Tetrahedron Lett.*, 1967, **8**, 2713.
40. (a) H. Tamaoki, R. Katoono, K. Fujiwara, and T. Suzuki, *Angew. Chem. Int. Ed*., 2016, **55**, 2582; (b) W. Nojo, H. Tamaoki, Y. Ishigaki, R. Katoono, K. Fujiwara, T. Fukushima, and T. Suzuki, *ChemPlusChem*, 2019, **84**, 634; (c) Y. Ishigaki, T. Harimoto, K. Sugimoto, L. Wu, W. Zeng, D. Ye, and T. Suzuki, *Chem. Asian J*., 2020, **15**, 1147.

41. (a) H. Wang and F. P. Gabbaï, *Angew. Chem. Int. Ed.*, 2004, **43**, 184; (b) H Kawai, T. Takeda, K. Fujiwara, M. Wakeshima, Y. Hinatsu, and T. Suzuki, *Chem. Eur. J.*, 2008, **14**, 5780; (c) T. Suzuki, Y. Yoshimoto, K. Wada, T. Takeda, H. Kawai, and K. Fujiwara, *Heterocycles*, 2010, **80**, 149.
42. T. Suzuki, A. Migita, H. Higuchi, H. Kawai, K. Fujiwara, and T. Tsuji, *Tetrahedron Lett.*, 2003, **44**, 6837.
43. (a) J. M. Seminario and J. M. Tour, *Ann. N. Y. Acad. Sci*., 1998, **852**, 68; (b) Y. Komoto, S. Fujii, M. Iwane, and M. Kiguchi, *J. Mat. Chem. C*, 2016, **438**, 8842; (c) A. Vilan, D. Aswal, and D. Cahen, *Chem. Rev*., 2017, **117**, 4248; (d) A. Vilan and D. Cahen, *Chem. Rev*., 2017, **117**, 4624; (e) D. Vuillaume, *ChemPlusChem*, 2019, **84**, 1215.
44. Reviews: (a) A. P. de Silva, H. Q. N. Gunaratne, and C. P. McCoy, *Nature*, 1993, **364**, 42; (b) S. Erbas-Cakmak, S. Kolemen, A. C. Sedgwick, T. Gunnlaugsson, T. D. James, J. Yoon, and E. U. Akkaya, *Chem. Soc. Rev.*, 2018, **47**, 2228.
45. F. M. Raymo, *Adv. Mater.*, 2002, **14**, 401.
46. T. Suzuki, S. Tanaka, H. Kawai, and K. Fujiwara, *Chem. Asian J.*, 2007, **2**, 171.
47. (a) M. M. Green, M. P. Reidy, R. J. Johnson, G. Darling, D. J. O'Leary, and G. Willson, *J. Am. Chem. Soc.*, 1989, **111**, 6452; (b) K. Obata, C. Kabuto, and M. Kira, *J. Am. Chem. Soc.*, 1997, **119**, 11345; (c) R. B. Prince, J. S. Moore, L. Brunsveld, and E. W. Meijer, *Chem. Eur. J*., 2001, **7**, 4150; (d) T. Suzuki, Y. Sakano, T. Iwai, S. Iwashita, Y. Miura, R. Katoono, H. Kawai, K. Fujiwara, Y. Tsuji, and T. Fukushima, *Chem. Eur. J.*, 2013, **19**, 117; (e) R. Katoono, S. Kawai, K. Fujiwara, and T. Suzuki, *Chem. Sci.*, 2015, **6**, 6592; (f) R. Katoono, K. Sakamoto, and T. Suzuki, *Chem. Commun.*, 2019, **55**, 5503.
48. (a) M. Tichý, M. Buděšínský, J. Günterová, J. Závada, J. Podlaha, and I. Císařová, *Tetrahedron*, 1999, **55**, 7893; (b) J. Vachon, C. Pérollier, D. Monchaud, C. Marsol, K. Ditrich, and J. Lacour, *J. Org. Chem.*, 2005, **70**, 5903.
49. F. Cozzi and J. S. Siegel, *Pure Appl. Chem*., 1995, **67**, 683.
50. (a) M. Nishio, M. Hirota, and Y. Umezawa, *The CH/π Interaction: Evidence, Nature, and Consequences*, Wiley-VCH, New York, 1998; (b) F. Ugozzoli, A. Arduini, C. Massera, A. Pochini, and A. Secchi, *New J. Chem*., 2002, **26**, 1718.
51. Y. Ishigaki, T. Iwai, Y. Hayashi, A. Nagaki, R. Katoono, K. Fujiwara, J. Yoshida, and T. Suzuki, *Synlett*, 2018, **29**, 2147.
52. T. Suzuki, K. Ohta, T. Nehira, H. Higuchi, E. Ohta, H. Kawai, and K. Fujiwara, *Tetrahedron Lett*., 2008, **49**, 772.
53. T. Suzuki, H. Tamaoki, K. Wada, R. Katoono, T. Nehira, and K. Fujiwara, *Chem. Commun*., 2012, **48**, 2812.

54. (a) R. Purrello, *Nat. Mat.*, 2003, **2**, 216; (b) L. Rosaria, A. D'Urso, A. Mammana, and R. Purrello, *Chirality*, 2008, **20**, 411.
55. Review: E. Yashima, N. Ousaka, D. Taura, K. Shimomura, T. Ikai, and K. Maeda, *Chem. Rev.*, 2016, **116**, 13752
56. K. Wada, Y. Chiba, T. Takeda, H. Kawai, R. Katoono, K. Fujiwara, and T. Suzuki, *Heterocycles*, 2014, **88**, 945.
57. T. Suzuki, K. Wada, Y. Ishigaki, Y. Yoshimoto, E. Ohta, H. Kawai, and K. Fujiwara, *Chem. Commun.*, 2010, **46**, 4100.
58. (a) T. Nehira, Y. Yoshimoto, K. Wada, H. Kawai, K. Fujiwara, and T. Suzuki, *Chem. Lett.*, 2010, **39**, 165; (b) T. Suzuki, Y. Yoshimoto, K. Wada, T. Takeda, H. Kawai, and K. Fujiwara, *Heterocycles*, 2010, **80**, 149; (c) T. Suzuki, H. Tamaoki, R. Katoono, K. Fujiwara, J. Ichikawa, and T. Fukushima, *Chem. Lett.*, 2013, **42**, 703.
59. T. Seki, T. Nakajo, and M. Onaka, *Chem. Lett.*, 2006, **35**, 824.
60. Y. Ishigaki, T. Shimajiri, T. Takeda, R. Katoono, and T. Suzuki, *Chem*, 2018, **4**, 795.
61. Y. Uchimura, T. Takeda, R. Katoono, K. Fujiwara, and T. Suzuki, *Angew. Chem. Int. Ed.*, 2015, **54**, 4010.
62. A. Schonberg and A. Mustafa, *J. Chem. Soc*., 1945, 657.
63. T. Suzuki, J. Nishida, M. Ohkita, and T. Tsuji, *Angew. Chem. Int. Ed*., 2000, **39**, 1804.
64. (a) W. Fenical, *J. Am. Chem. Soc.*, 1974, **96**, 5580; (b) Y. Takahashi, M. Ando, and T. Miyashi, *Tetrahderon Lett.*, 1995, **36**, 1889; (c) Y. Ushigoe, Y. Torao, A. Masuyama, and M. Nojima, *J. Org. Chem*., 1997, **62**, 4949; (d) A. V. Arzumanyan, R. A. Novikov, A. O. Terent'ev, M. M. Platonov, V. G. Lakhtin, D. E. Arkhipov, A. A. Korlyukov, V. V. Chernyshev, A. N. Fitch, A. T. Zdvizhkov, I. B. Krylov, Y. V. Tomilov, and G. I. Nikishin, *Organometallics*, 2014, **33**, 2230; (e) P. S. Radulov, Yu. Yu. Belyakova, A. A. Demina, G. I. Nikishin, I. A. Yaremenko, and A. O. Terent'ev, *Russ. Chem. Bull.*, 2019, **68**, 1289.
65. Y. Ishigaki, M. Takata, and T. Suzuki, *The 10th CSJ Festa Abstract Book*, 2020, A201074.
66. T. Suzuki, T. Kuroda, H. Tamaoki, S. Higasa, T. Nehira, R. Katoono, Y. Ishigaki, K. Fujiwara, T. Fukushima, and H. Yamada, *Heterocycles*, 2017, **95**, 816.
67. After submission of this review, an interesting application of bis(xanthenyl) compounds has been reported which enables reduction of oxygen via the endoperoxides with two spiro(xanthene)s: M. Karimi, R. Borthakur, C. L. Dorsey, C.-H. Chen, S. Lajeune, and F. P. Gabbaï, *J. Am. Chem. Soc.*, 2020, **142**, 13651.
68. E. Ohta, T. Nehira, H. Kawai, K. Fujiwara, and T. Suzuki, *Tetrahedron Lett.*, 2008, **49**, 777.

Takanori Suzuki was born in Miyagi Prefecture, Japan in 1961. He graduated from Tohoku University in 1984 and received his Ph.D. in 1988 under the supervision of Professors Toshio Mukai and Tsutomu Miyashi. After he worked at Tohoku University as a JSPS post-doctoral fellow for 1988-1989 and as Research Associate for 1989-1994, he moved to Faculty of Science, Hokkaido University and joined Professor Takashi Tsuji's group as Associate Professor (1995-2002). He was appointed as Professor at Hokkaido University in 2002. He received The Chemical Society of Japan Award for Young Chemists for 1996, 1st Nozoe Memorial Award for Young Chemists (2004), and The Chemical Society of Japan Award for Creative Work for 2019. He has been working in the area of structural and physical organic chemistry, and his main themes are the studies on dynamic redox systems, construction of record-breaking strained compounds, and development of unimolecular memory.

Yusuke Ishigaki was born in Obihiro (Hokkaido), Japan, in 1985. He graduated from Hokkaido University in 2008 and received his Ph.D. in 2012 under the supervision of Professor Takanori Suzuki. After he worked as a JSPS postdoctoral fellow at Ulm University (Professor Peter Bäuerle) and at Nippon Steel & Sumikin Chemical Co., Ltd., he moved to Hokkaido University as an assistant professor in 2016. He received the Encouragement Award from Hokkaido Branch of The Chemical Society of Japan (2020), and Special Lecturer for Young Chemists in the 100th CSJ Annual Meeting (2020). His research interests include flexible C–C covalent bond such as long C–C single bond (hyper covalent bond) and strained C=C double bond-based redox-active molecules.

Masaki Takata was born in Hyogo Prefecture, Japan in 1997. He entered Kwansei Gakuin University in 2016, and started his research on organic chemistry with Prof. Hidetoshi Yamada in 2019. He received Bachelor of Science degree in 2020 from Kwansei Gakuin University. He is currently master’s course student in Prof. Suzuki’s laboratory at Hokkaido University.

Jun-ichi Nishida was born in Kyoto Prefecture, Japan in 1973. He graduated from Hokkaido University in 1996 and received his Ph.D. in 2001 under the supervision of Professors Takanori Suzuki and Takashi Tsuji. He worked as a JSPS post-doctoral fellow in 1998-2001. After he graduated University, he moved to Interdisciplinary Graduate School of Engineering, Tokyo Institute of Technology, and joined Professor Yoshiro Yamashita's group as Assistant Professor (2001-2013). He moved to Department of Applied Chemistry, University of Hyogo as Associate Professor in 2013. He won a student poster award at Pacifichem in 2000. He has been working in the area of structural and physical organic chemistry, and his main themes are the studies on redox active molecules applicable to organic electronics.

Takanori Fukushima was born in Tochigi Prefecture, Japan in 1969. He graduated from Tohoku University in 1992 and received his Ph.D. in 1999 under the supervision of Professor Tsutomu Miyashi. In the period of 1995–1996, he worked as a JSPS research fellow and began his academic career as a research associate at Tohoku University from 1996. In 2001, he moved to ERATO Aida Nanospace Project, Japan Science and Technology Agency (JST), as a researcher and became a group leader in 2004. In 2007, he was appointed as a team leader of Functional Soft Matter Research Group in RIKEN Advanced Science Institute. In 2010, he was appointed as a full professor at Tokyo Institute of Technology. His has been working in the areas of physical organic chemistry, supramolecular chemistry, and polymer chemistry, and his recent research interest focuses on the design of functional organic and polymer materials based on controlled molecular self-assembly. He received awards including The Wiley Award (2005) from The Society of Polymer Science Japan, and the Young Scientists' Prize (2008) and the Science and Technology Prize, Research Category (2020), The Commendation for Science and Technology by the Minister of Education, Culture, Sports, Science and Technology.